電気学会論文誌 A（基礎・材料・共通部門誌）
IEEJ Transactions on Fundamentals and Materials
Vol.136 No.2 pp.99-104 DOI: 10.1541/ieejfms.136.99

Paper

Visualization of Spatially Distributed Bioactive Molecules using Enzyme-Linked Photo Assay

Hikaru Mabuchi* Student Member, HongYao Ong* Associate
Kazunori Watanabe* Non-member, Sachiko Yoshida* Non-member
Naohiro Hozumi*a) Senior Member

(Manuscript received March 18, 2015, revised Oct. 4, 2015)

In this paper, we propose a new simple device for visualizing bioactive molecules with a fine spatial resolution by using a membrane in which a specific enzyme is immobilized. The layer produces fluorescence after association with a specific substance. The layer, on which a biological tissue is to be mounted, is deposited on a quartz substrate that is used as a light guide to introduce UV light to the layer. Substance release is observed by a CCD camera from the opposite side of the substrate. In order to shorten the experiment time, we had automated the optical device. The paper also describes the reduction of background fluorescence by means of image processing technique. Images were acquired by employing two UV-LEDs with slightly different angle. Image processing was performed to separate background and target fluorescence by means of independent component analysis. Finally the release of GABA(γ-aminobutyric acid) and glutamate from specific layers in rat cerebellum was successfully observed. It is expected that, using this method, both real-time transmitter release and its response to medicine can be observed.

Keywords : bioactive molecules, enzyme-linked photo assay, independent component analysis

1. Introduction

Light guide is composed of a dielectric material that can enclose the light propagation. In addition to being applied to communication, it is useful for sensing as well. In chemical sensing the surface of the light guide has to be coated with some specific chemical that may change its optical property depending on chemical reactions. Such a function can be applied to chemical imaging, if the light guide has a flat surface. This study proposes an application of two-dimensional light guide, of which surface is chemically modified, to biochemical imaging.

Neurotransmitter molecules released from neurons are not only regulators of neuronal transduction but also indicators of neuronal conditions. Glutamate and γ-aminobutyric acid (GABA) are known as typical transmitters in brain cortex that play important roles as stimulator and suppresser, respectively. Lack of balance in the release of glutamate and GABA may lead to autism, epilepsy or Parkinson's disease[1][2].

In order to observe the spatio-temporal release in cerebellar cortex, we have newly proposed the enzyme-linked photo assay system, which is realized even using normal CCD camera, and observed GABA release in developing cerebellar slice using either new or authorized methods[3].

In this paper, we propose a new simple device for this purpose by using a reactive layer in which a specific enzyme is immobilized, and produces fluorescence after association with a specific substance released from mounted slice. This layer is bound a quartz substrate that is used as a light guide for UV light excitation. Fluorescence derived from a substance is observed by a CCD camera from the opposite side of the substrate.

The paper describes the reduction of background fluorescence by means of image processing technique. Finally it will be shown that the release of transmitters from specific layers in rat cerebellum was successfully observed.

2. Specimen Preparation and Photo Excitation System

Imaging of neurotransmitter release was monitored the reaction of oxidoreductases generating reduced nicotinamide adenine dinucleotide (NAD^+) or diphosphonucleotide ($NADP^+$). For glutamate and GABA, we used glutamate dehydrogenase and GABA disassembly enzyme (GABase), respectively.

Enzymes were covalently immobilized on the quartz glass substrate using a silane coupling agent and a crosslink agent. The substrate was as thick as 1 mm. Stoichiometrically generated NADH or NADPH emits 480 nm fluorescence after excitation at 340-365 nm.

Existence of glutamate and GABA lead to fluorescence when co-existing with specific enzyme and co-enzyme. A glass substrate on which specific enzyme is coated is in contact with the biological specimen. A chamber space is created around the specimen. The space is filled with buffer liquid and co-enzyme. On the glass substrate therefore, the specimen is in contact with both enzyme and co-enzyme.

Consequently glutamate or GABA, that is released from the tissue spontaneously by stimulation, makes an oxidation-reduction reaction on the substrate. Although both glutamate and GABA do not produce fluorescence by themselves, NAD(P)H that is created as the result of the above chemical reaction makes fluorescence. As the ratio of glutamate or GABA and NAD(P)H is 1:1, the

a) Correspondence to: Naohiro Hozumi. E-mail: hozumi@icceed.tut.ac.jp
* Toyohashi University of Technology
1-1, Hibarigaoka, Tenpaku, Toyohashi 441-8580, Japan

© 2016 The Institute of Electrical Engineers of Japan.

fluorescence can be correlated to the amount of released glutamate or GABA.

In the experiment, rat cerebellum was sliced sagittally at 400 μm thick and incubated in oxygen-aerated HEPES-Na^+ buffer for 40 min. The slice was placed on the quartz glass substrate with both $NADP^+$ and α-ketoglutarate. Figure 1 shows the schematic diagram of the observation system including the device. The enzyme was immobilized covalently on the glass as shown in Fig. 2. Figure 3 shows chemical reactions taking place on the substrate. $NADP^+$ (nicotinamide adenine dinucleotide phosphate) changes into NADPH (reduced nicotinamide adenine dinucleotide phosphate) just as glutamate and GABA degeneration. Synthesized NADPH was illuminated by 360 nm surface UV-LED, and emitted the 480 nm fluorescent light observed by cooled CCD (ORCA ER, Hamamatsu Photonics). The quartz substrate can be recognized as a light guide to illuminate the surface of the substrate.

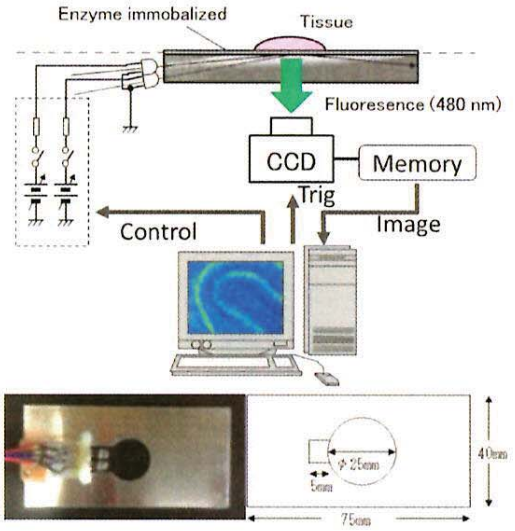

Fig. 1. Schematic diagram of the observation system including the device and its outlook

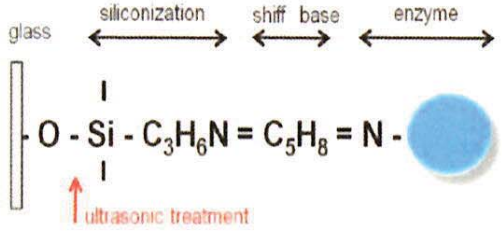

Fig. 2. Immobilized enzyme

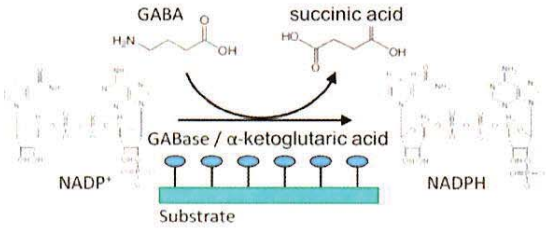

Fig. 3. Chemical reaction on the substrate

3. Image Processing

The fluorescent light detected by the CCD camera is divided into target light and background light. As significant intensity of background light is detected, it is assumed that fluorescence is excited by the light that is refracted on the interface between the substrate and tissue system including the layer. The light, being generated by LEDs and propagates though the substrate, can be decomposed into plane waves with different angles of propagation. Each plane wave transfers across the enzyme layer and comes into the tissue. We assume that both target and background light were predominantly excited by normal light. As the background light significantly damage the quality of the image, it should be reduced as much as possible. Making use of the evanescent light may be a solution, however, it may make the system complicated, and the target light may be not as significant as this case. Therefore we tried to reduce the background by means of a simple image processing.

Assuming that the light is a plane wave and scatter can be neglected, wave propagation and detected fluorescence can be illustrated as Fig. 4. In the figure, fluorescence, attributed to the layer where the enzyme is fixed, is represented as I_0. This is

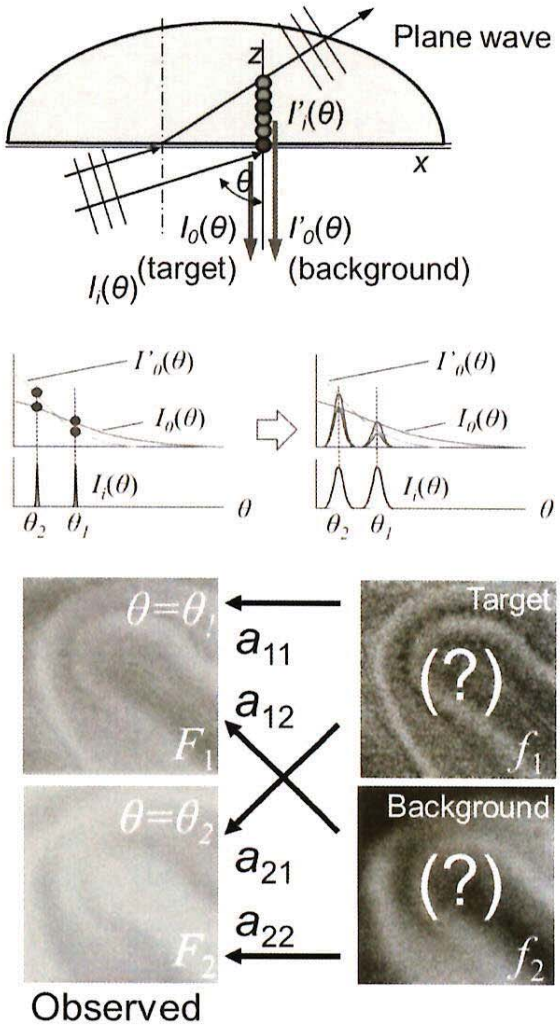

Fig. 4. Fluorescence detected by CCD camera

defined as to be the target. The fluorescence attributed to the tissue is represented as I'_0. This is defined as to be the background. Both I_0 and I'_0 depends on the incident angle θ. The thickness of the quartz plate, which is used as a light guide, is as thick as 1 mm. As it is much thicker than the diameter of normal optical fiber it is relatively easy to introduce two kinds of lights of which angles of center axes are significantly different. In addition, in practice, they depend differently on the incident angle. As the result, the proportion (I_0/I'_0) is not the same along θ. This is true even if the incident angle has distributed.

As the result, the captured fluorescence with different angle of optical axis is composed of target and background fluorescence with different mixture ratios. This can be represented as:

$$\begin{pmatrix} F_1 \\ F_2 \end{pmatrix} = \begin{pmatrix} a_{11} & a_{12} \\ a_{21} & a_{22} \end{pmatrix} \begin{pmatrix} f_1 \\ f_2 \end{pmatrix} \quad \cdots\cdots (1)$$

where $F_1(x,y)$ and $F_2(x,y)$ are captured fluorescence image, $f_1(x,y)$ and $f_2(x,y)$ are spatial distributions of fluorescence as the target and background, a_{11}, a_{12}, a_{21}, a_{22} are constants. Although the image acquisition is sequential, ICA is performed by assuming that two images, $F_1(x,y)$ and $F_2(x,y)$ are acquired with a negligible time lag. Reproduced images $f'_1(x,y)$ and $f'_2(x,y)$ are calculated from F_1 and F_2. As the result of periodical acquisitions of F_1 and F_2, time dependent images of f'_1 and f'_2 are calculated. Eq. (1) can also be described using a matrix expression as:

$$\mathbf{F} = \mathbf{A} \cdot \mathbf{f} \quad \cdots\cdots (2)$$

The target and background fluorescence distribution can be calculated by applying $\mathbf{A}^{-1}$ to $\mathbf{F}$. In practice, only contrast of the image would be enough to recognize the distribution. In such a case $\mathbf{A}^{-1}$ can be represented as:

$$\begin{pmatrix} 1 & \alpha \\ \beta & 1 \end{pmatrix} \quad \cdots\cdots (3)$$

After capturing two images $\mathbf{F}_1$ and $\mathbf{F}_2$ by changing the angle of optical axis, the target and background images can be separated by finding appropriate numbers for α and β. α and β can be tuned manually by monitoring the quality of reproduced image, however, the theory of independent component analysis (ICA) may be powerful for solving such a problem[4].

Stochastic distribution of pixel intensity in images f'_1 and f'_2 are represented as $p(y_{1i})$ and $p(y_{2j})$, where y_{1i} and y_{2j} represent the intensity.

$$\left.\begin{aligned} p(y_1) &\equiv \{p(y_{11}), \cdots, p(y_{1i}), \cdots p(y_{1n})\} \\ p(y_2) &\equiv \{p(y_{21}), \cdots, p(y_{2j}), \cdots p(y_{2n})\} \end{aligned}\right\} \quad \cdots\cdots (4)$$

$p(y_{1i}, y_{2j})$ represents the probability that the intensity of a pixel in image f'_1 is y_{1i} and that of the corresponding point in image f'_2 is y_{2j}. In other words $p(y_1)$ and $p(y_2)$ are probabilities that cases y_1 and y_2 take place, respectively, and $p(y_1, y_2)$ is the probability that cases y_1 and y_2 takes place simultaneously. Variables y_1 and y_2 are considered to be independent when

$$p(y_1, y_2) = p(y_1)p(y_2) \quad \cdots\cdots (5)$$

is established. Kullback-Leibler (K-L) parameter is often employed to indicate the independency of variables:

$$KL \equiv \sum_{i,j} p(y_{1i}, y_{2j}) \log \frac{p(y_{1i}, y_{2j})}{p(y_{1i})p(y_{2j})} \quad \cdots\cdots (6)$$

The K-L parameter is zero when two sets of variables y_1 and y_2 are completely independent together. In practice, α and β in Eq. (3), which determine the probabilities $p(y_1)$, $p(y_2)$ and $p(y_1, y_2)$, can be tuned so that the K-L parameter indicates the minimum.

The process of ICA is illustrated in Fig. 5. The equation described in the form of matrix indicates that two images, F_1 and F_2, derive from linear combination of unknown original images f_1 and f_2. If an appropriate inverse matrix can be found then the original images can be reproduced. However as the matrix to describe the linear combination is unknown as well, ICA algorithm is applied to find the most appropriate matrix (as the inverse matrix). In the

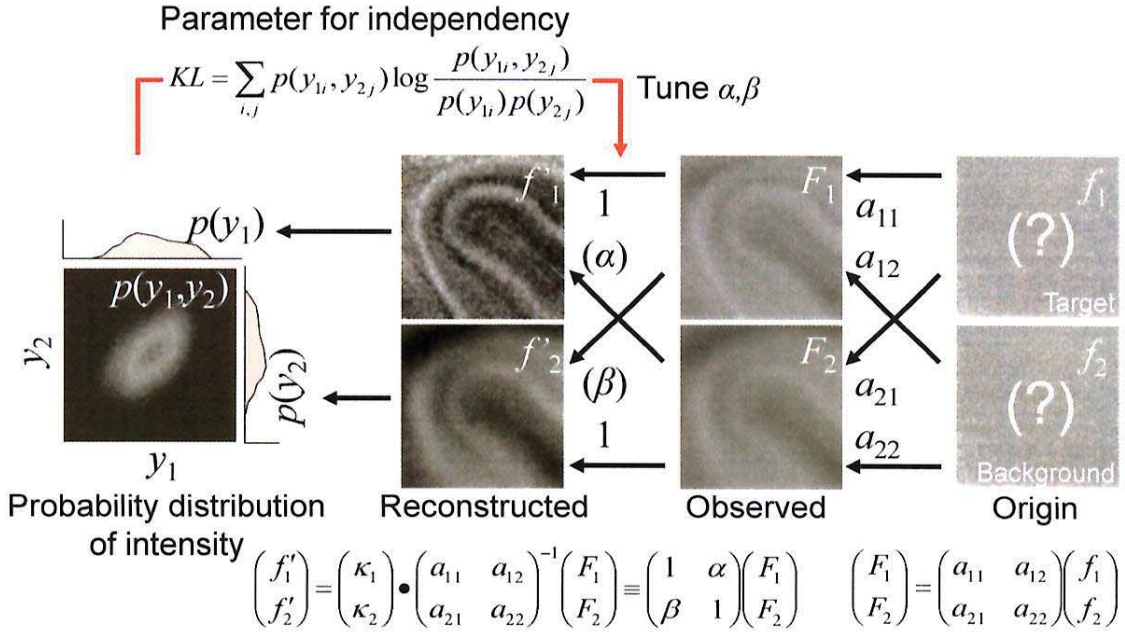

Fig. 5. Illustration for image processing based on independent component analysis

ICA process K-L parameter is calculated in order to evaluate the probabilistic independency of images f'_1 and f'_2. It can be considered that in the reproduction algorithm the core process is the calculation of the K-L parameter. In this preliminary study K-L parameter is successively calculated by manually changing the inverse matrix, and images are assumed to be reproduced when the K-L parameter indicates the minimum.

4. Results and Discussion

4.1 Image Processing using the ICA Figure 6 (a) shows visible light image of the cerebellum with postnatal 21 days. In developing cerebellum, granule cells, small input neurons, proliferate and migrate down from the external granular layer (EGL) to the internal granular layer (IGL). As the development proceeds, EGL turns into molecular layer (ML) whereas IGL remains. Purkinje cells, big output neurons, develop their dendrites and associate neuronal connections between granule cells and other interneurons. Neuronal circuit layer forms the ML. As the cerebellum shown in Fig. 6 (a) is mature, ML, PL, IGL are clearly visible. Note that ML is on the outer side of the cerebellum, and a wrinkle surrounded by the ML is seen in Fig. 6 (a).

As for fluorescence observation, three different images were acquired. Two were with different inclination of the excitation light source, and one was with no excitation light. Each of the two images with excitation light was subtracted with the image with no excitation light, in order to reduce the background light from the outside. These two images after the subtraction were defined as images A and B.

Figure 6 (b) shows these images for a rat cerebellum. Both images are very unclear, because of the background fluorescence. Figure 6 (c) shows the result of image processing. It is clearly shown in the image entitled as "target" that the fluorescence intensity is high in two layers, whereas that entitled as "background" is not clear. By morphological inspection these layers are recognized as ML and IGL. These layers are known that GABAergic neurons distribute in mature cerebellum. Studies using HPLC and electrophysiological method have shown that GABA is released from the postnatal cerebellar cortex even before synaptogenesis, and that GABA receptors act on the developing cerebellar Purkinje cells[4][5]. However, dynamic GABA release could not be observed unless the enzyme-linked photo assay is used. In addition, because cytoplasmic autofluorescence becomes noisy background light, it is useful that the image processing system extracted the image of GABA release from the autofluorescence-contained image. Using this method, both real-time transmitter release and its response to medicine can be observed.

4.2 Transition after Chemical Stimulation In relatively developed cerebellum, cells distributed in the ML and IGL are only the neurons of glutamate release, so that both layers showed fluorescent activities. Figure 7 indicates release distribution of glutamate in comparison with normal optical image illuminated with visible light. The fluorescent image, indicating glutamate release, is after the ICA processing. Figure 7 (c) indicates the regions of interest for analysis. Regions highlighted as ML and IGL have relatively strong intensity in fluorescence. They have a contrast to the region highlighted as PL. Release from white matter (WM), which is mostly composed of fatty materials, is much less significant.

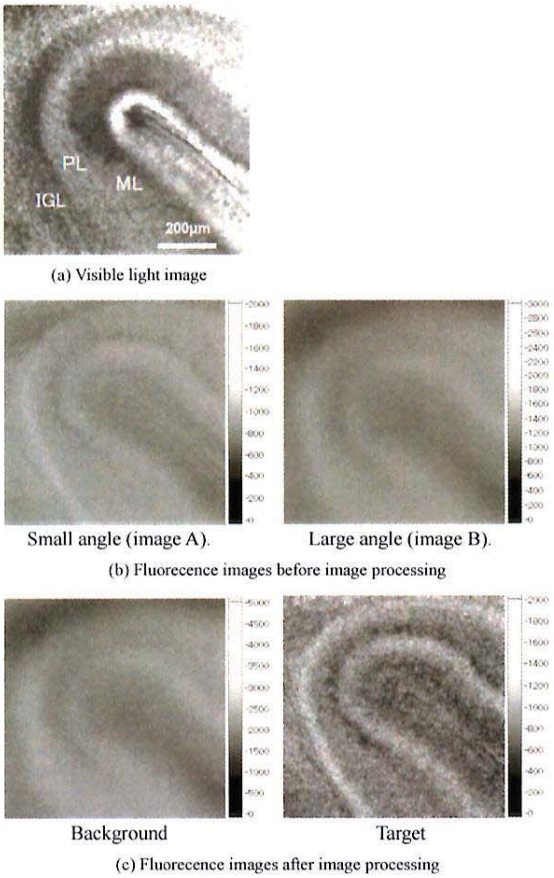

(a) Visible light image

(b) Fluorecence images before image processing

(c) Fluorecence images after image processing

Fig. 6. Cross sectional mages of cerebellar cortex: (a) Visible light image, (b) original fluorescent images with different angle of optical axes, and (c) fluorescent images after the image processing. Scales are indicated in arbitrary unit. Specimen: rat cerebellum (postnatal 21 days), target: GABA

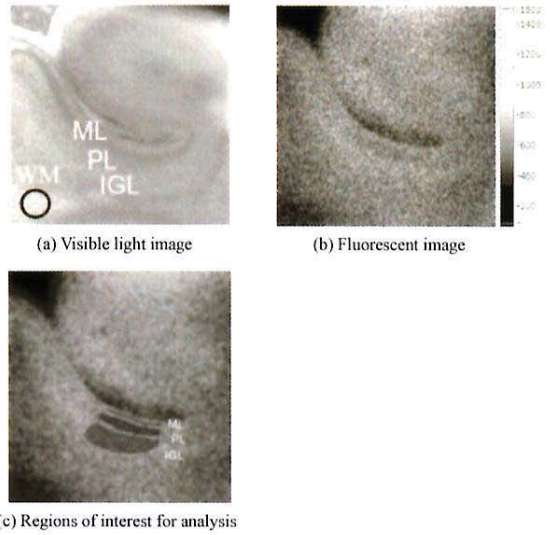

(a) Visible light image

(b) Fluorescent image

(c) Regions of interest for analysis

Fig. 7. Cerebellum with postnatal 7 days observed with visible light and fluorescent light indicating glutamate release. 0.9 mm × 0.9 mm. Gray scale is arbitrary. ML: molecular layer, PL: Purkinje layer, IGL: internal granular layer, WM: white matter. Specimen: rat cerebellum (postnatal 7 days)

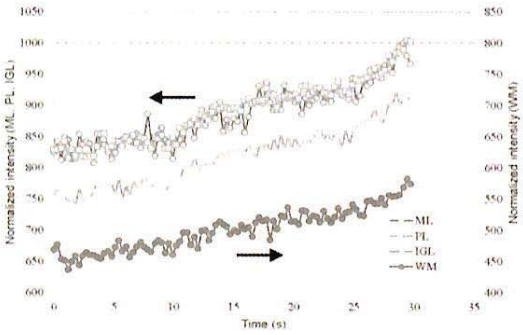

Fig. 8. Transition in fluorescence intensity in each layer (normalized by the intensity of ML 30 s after stimulation that is indicated as 1000). Specimen: rat cerebellum (postnatal 7 days), target: glutaminate

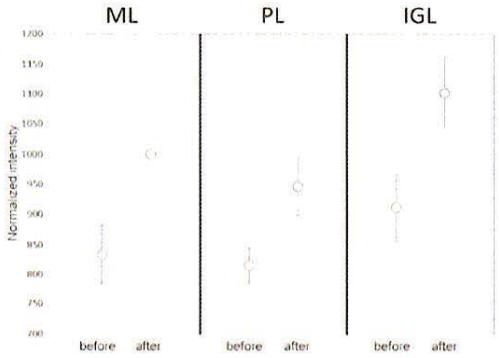

Fig. 9. Change in fluorescence intensity before and after AMPA stimulation (normalized by the intensity of ML 30 s after stimulation that is indicated as 1000). Specimen: rat cerebellum (postnatal 7 days), target: glutaminate

Our system can visualize both spontaneous and responsive transmitter release with about 0.2 s time resolution. Figure 8 shows the transition of glutamate release in response to 100 μmol/ℓ (S)-alpha-Amino-3-hydroxy- 5 methylisoxazole-4-propionic acid (AMPA) application in cerebellar slices. All values are normalized by the intensity of ML 30 s after stimulation that is indicated as 1000. Fluorescence, as indication glutamate release, was intense in both the IGL and ML, whereas the PL was indicated with lower intensity. As shown in Fig. 8, a clear increase in fluorescence was observed after stimulation. Transition in fluorescence was similar for ML and IGL, suggesting that these layers are activated. However PL, which was not expected to release glutamate, showed fluorescence as well although it was less intense than ML and IGL. As this specimen was taken from relatively young rat (postnatal 7 days), the cerebellar development was not totally completed, and the layers were not separated enough. It is hence considered that diffusion from ML and IGL to PL would take place, leading to an increase in fluorescence in this layer. The increase in fluorescence in WM suggests that glutamate might have been diffused into WM as well, although the absolute value was much lower than ML and IGL.

Figure 9 compares the fluorescence in each layer before and after stimulation. Four different specimens were used for the observation, in order to confirm reproducibility. It is clear that the AMPA stimulation brought a significant glutamate release from ML and IGL, although the increase is also seen with PL.

5. Conclusions

A new method for visualization of spatially distributed bioactive molecules using enzyme-linked photo assay has been proposed. It is based on fluorescent reaction assisted by an enzyme immobilized on the substrate, however, background fluorescence disturbs the observation. In order to reduce the background fluorescence, two images were acquired by changing the optical axis of UV illumination. Image processing based on independent component analysis made the target image clear. Observation of rat cerebellum was successfully performed and GABA and glutamate release from two specific layers was clearly indicated.

Acknowledgement

The study was partially supported by grants from Scientific Research (C) 23500516, 26350498 and Health Labor Sciences Research.

References

(1) N. C. Danbolt : "Glutamate Uptake", *Neurobiology*, Vol.65, pp.1-105 (2001)
(2) N. Kasai, Y. Jimbo, O. Niwa, T. Matsue, and K. Torimitsu : "Rea-time Multisite Observation of Glutamate Release in Rat Hippocampal Slices", *Neurosdence Lett.*, Vol.304, pp.112-116 (2001)
(3) T. Morishima, M. Uematsu, T. Furukawa, Y. Yanagawa, A. Fukuda, and S. Yoshida : "GABA Imaging in Brain Slices Using Enzyme-linked Photo Analysis", *Neurosci. Res.*, Vol.67, pp.347-353 (2001)
(4) V. Calhoun, G. Pearlson, and T. Adali : "Independent Component Analysis to fMRI Data, A Generative Model for Validating Results", VLSI Signal Processing, Vol.37, pp.281-291 (2004)
(5) F. F. Trigo, M. Chat, and A. Marty : "Enhancement of GABA Release through Endogenous Activation of Axonal GABA(A) Receptors in Juvenile Cerebellum", *J. Neurosci.*, Vol.27, No.46, pp.12452-63 (2007)
(6) K. Obata : "Excitatory and Trophic Action of GABA and Related Substances in Newborn Mice and Organotypic Cerebellar Culture", *Dev Neurosci*, Vol.19, No.1, pp.117-119 (1997)

Hikaru Mabuchi

(Student Member) was born in Hokkaido, Japan on July 25, 1992. He is 1st-year student in Graduate School of Toyohashi University of Technology. His major is electric and electronic information. He has been engaged in research on bio-sensing by means of optical measurement. He is a student member of IEEJ.

HongYao Ong

(Associate) was born in Malaysia on June 30, 1990. He received his B.S degree in 2014 from Toyohashi University of Technology, Japan. His major is electric and electronic information. He is currently engaged in GS Reality Sdn. Bhd., Malaysia. His major is electric and electronic information. He is an associate member of IEEJ.

Kazunori Watanabe

(Non-member) was born in Asahikawa, Japan on February 3, 1992. He is 2nd-year student in Graduate School of Toyohashi University of Technology. His research focuses both the optimization of surface modification for biosensor, and detection of neurotransmitters. He is a member of Japan neuroscience Society.

Sachiko Yoshida

(Non-member) was born in Toyama, Japan on January 24, 1961. She received her B.S., M.S. and Ph.D. degrees in 1983, 1986 and 1990 from University of Tokyo. She was engaged in JSPS Postdoctoral Researcher from 1990 to 1992, JST PRESTO Researcher from 1992 to 1994, and Research Associate at Toyohashi University of Technology from 1995 to 1996. Since 1996, she has been a lecturer of Toyohashi University of Technology. Her research interests focus the physiological interaction and morphological transformation through brain differentiation, and these detections. She is a member of a member of IEEE, International Brain Research Organization, Society for neuroscience, Japan neuroscience Society, and the Physiological Society of Japan.

Naohiro Hozumi

(Senior Member) was born in Kyoto, Japan on April 2, 1957. He received his B.S., M.S. and Ph.D. degrees in 1981, 1983 and 1990 from Waseda University. He was engaged in Central Research Institute of Electric Power Industry (CRIEPI) from 1983 to 1999. He was an associate professor of Toyohashi University of Technology from 1999 to 2006, and a professor of Aichi Institute of Technology from 2006 to 2011. Since 2011, he has been a professor of Toyohashi University of Technology. He has been engaged in the research in insulating materials and diagnosis for high voltage equipment, acoustic measurement for biological and medical applications, etc. He was awarded in 1990 and 1999 from IEE of Japan for his outstanding research papers. He is a member of IEEE, IEE of Japan and the Acoustic Society of Japan.

J Occup Health 2016; 58: 241-246

Journal of Occupational Health

Original

A cross-fostering analysis of bromine ion concentration in rats that inhaled 1-bromopropane vapor

Toru Ishidao[1], Yukiko Fueta[1], Susumu Ueno[2], Yasuhiro Yoshida[3] and Hajime Hori[1]

[1]Department of Environmental Management, School of Health Sciences, University of Occupational and Environmental Health, Japan, [2]Department of Occupational Toxicology, Institute of Industrial Ecological Sciences, University of Occupational and Environmental Health, Japan and [3]Department of Immunology and Parasitology, School of Medicine, University of Occupational and Environmental Health, Japan

Abstract: Objective: Inhaled 1-bromopropane decomposes easily and releases bromine ion. However, the kinetics and transfer of bromine ion into the next generation have not been clarified. In this work, the kinetics of bromine ion transfer to the next generation was investigated by using cross-fostering analysis and a one-compartment model. **Methods:** Pregnant Wistar rats were exposed to 700 ppm of 1-bromopropane vapor for 6 h per day during gestation days (GDs) 1-20. After birth, cross-fostering was performed between mother exposure groups and mother control groups, and the pups were subdivided into the following four groups: exposure group, postnatal exposure group, gestation exposure group, and control group. Bromine ion concentrations in the brain were measured temporally. **Results:** Bromine ion concentrations in mother rats were lower than those in virgin rats, and the concentrations in fetuses were higher than those in mothers on GD20. In the postnatal period, the concentrations in the gestation exposure group decreased with time, and the biological half-life was 3.1 days. Conversely, bromine ion concentration in the postnatal exposure group increased until postnatal day 4 and then decreased. This tendency was also observed in the exposure group. A one-compartment model was applied to analyze the behavior of bromine ion concentration in the brain. By taking into account the increase of body weight and change in the bromine ion uptake rate in pups, the bromine ion concentrations in the brains of the rats could be estimated with acceptable precision.

Received October 21, 2015; Accepted December 18, 2015
Published online in J-STAGE April 22, 2016
Correspondence to: Toru Ishidao, Department of Environmental Management, School of Health Sciences, University of Occupational and Environmental Health, 1-1 Iseigaoka, Yahatanishi-ku, Kitakyushu, 807-8555, Japan (e-mail: ishidao@health.uoeh-u.ac.jp)

(J Occup Health 2016; 58: 241-246)
doi: 10.1539/joh.15-0284-OA

Key words: 1-Bromopropane inhalation, Cross-fostering, Bromine ion concentration, One-compartment model, Animal experiment

1-Bromopropane (1-BP, CAS no. 106-94-5) is widely used as a substitute for chlorofluorocarbons, which destroy the ozone layer. The toxicity of 1-BP has been reviewed[1], and the Japan Society for Occupational Health recommends an occupation exposure limit of 0.5 ppm[2]. Previously, we studied the effects of inhaled 1-BP vapor in male rats on the nervous[3-8] and immune systems[9,10].

We also studied the effects of inhaled 1-BP vapor on metabolism in male rats and reported that 1-BP rapidly decomposes and releases bromine ion in the blood[11], indicating that bromine ion is a major index of 1-BP exposure. Recently, because of the health effects reported in female workers exposed to 1-BP[12-14], there is concern regarding the health effects of 1-BP exposure on the next generation. Some researchers have reported results of experiments in female animals[15-17]; however, the kinetics of bromine ion distribution to the next generation has not been elucidated. In this study, pregnant rats were exposed to 700 ppm of 1-BP vapor, and the concentration of bromine ion in the rat brain was measured. The distribution of bromine in fetuses and cross-fostered pups was investigated. A one-compartment model was employed to analyze the behavior of bromine ion in rats.

Methods

Animals

Female (9-week-old) and male (10-week-old) Wistar rats were purchased from Kyudo Co., Ltd. (Saga, Japan). After acclimation in polycarbonate cages with dry chips,

Table 1. Experimental groups and ages of adult and fetal rats exposed to 700 ppm of 1-BP and of pups on sampling day

Groups (n)		Age (n) on sampling day
Virgin female	Exposure (5)	GD21 (2)
Mother	Exposure (11)	GD20 (3)
	Control (5)	
Fetus	Exposure	GD20 (13)
Pup†	Exposure	PND1 (10), PND3 (10), PND5 (5), PND7 (5)
	Postnatal exposure	PND2 (5), PND4 (5), PND8 (5)
	Gestation exposure	PND4 (5), PND8 (5)
	Control	PND3 (5)

1-BP: 1-bromopropane, GD: gestation day, PND: postnatal day, †: Exposure=1-BP exposed pups were raised by their birth mother exposed to 1-BP, Postnatal exposure=control pups were raised by 1-BP exposed mother, Gestation exposure=1-BP exposed pups were raised by control mother, Control=control pups were raised by control mother

they were housed in pairs in animal rooms under 12-h light-dark cycle conditions at 22 ± 1℃ and 55 ± 5% relative humidity, with free access to food and water. The presence of sperm in the vaginal smear was defined as day 0 of gestation (GD0; female rats were 11 weeks old). In the inhalation study, the female rats were divided into three groups: 1-BP-exposed virgin female group (n=5), 1-BP-exposed mother group (n=11), and the control mother group (n=5). After the final exposure of mother rats on GD20, they were housed in an animal room for the onset of birth. Postnatal day (PND) i.e., the day after birth, was defined as day 0 (PND0=GD21). On PND1, a litter size of eight pups was assembled and cross-fostering[17,18] of pups was performed between mother exposure groups (n=3) and mother control groups (n=3). The pups were subdivided into four groups: (1) exposure group (1-BP-exposed pups were raised by their birth mother exposed to 1-BP), (2) postnatal exposure group (control pups were raised by 1-BP-exposed mother), (3) gestation exposure group (1-BP-exposed pups were raised by control mother), and (4) control group (control pups were raised by their control mother). The experimental groups are summarized in Table 1. Body weight was measured periodically. The experiments were conducted per the guidance of the Ethics Committee of Animal Care and Experimentation in accordance with The Guiding Principle for Animal Care Experimentation, University of Occupational and Environmental Health, Japan (AE03-065), which conforms to the National Institutes of Health Guide for the Care and Use of Laboratory Animals and the Japanese Law for Animal Welfare and Care.

Exposure

Reagent-grade 1-BP was obtained from Kanto Chemical Co., Ltd. (Tokyo, Japan). 1-BP vapor was introduced into a 400-*l* stainless-steel exposure chamber. Details of this apparatus and procedure have been given elsewhere[11]. In order to study change in bromine ion in blood and brain when the condition of dysfunction of feedback inhibition (i.e., disinhibition) was confirmed, exposure concentration was designed to be 700 ppm, which was higher than LOAEL (400 ppm) for disinhibition[7]. The actual concentration of 1-BP vapor in the chamber was 701.3 ± 5.2 ppm. In the control group, only clean air was introduced into the chamber. The exposure period was 6 h per day between 9 a.m. and 3 p.m. throughout gestation or GD 1-20 (virgin female group was exposed until GD21). Table 1 displays the age of the rats on sampling day. They were deeply anesthetized with diethyl ether and then decapitated. The brains and the stomachs with milk from only the exposure group on PND1 were gently removed and stored in a freezer.

Measurement of bromine ion concentration

The brains (cerebrum and diencephalon) and stomachs (0.25 g) were homogenized with water (1.5 m*l*) at 0℃. The sample (1 m*l*) was dispensed into a vial, and 0.1 m*l* of dimethyl sulfate was added to convert bromine ion to methyl bromide. Then, 0.1 m*l* of an aqueous solution of isopropyl alcohol (0.5 volume percent) was added as an internal standard. The vial was heated at 50℃ for 1 h. The bromine ion concentration was determined by measuring peak area of methyl bromide vapor in the headspace by using a gas chromatograph mass spectrometer (GC/MS, QP-5050; Shimadzu, Kyoto, Japan)[11].

Estimation method of bromine ion concentration

As previously described, inhaled 1-BP was metabolized and bromine ions were released. In this study, the behavior of released bromine ion concentration in the brain was analyzed by using a one-compartment model[19]. We assumed the bromine ion uptake rate, i.e., the genera-

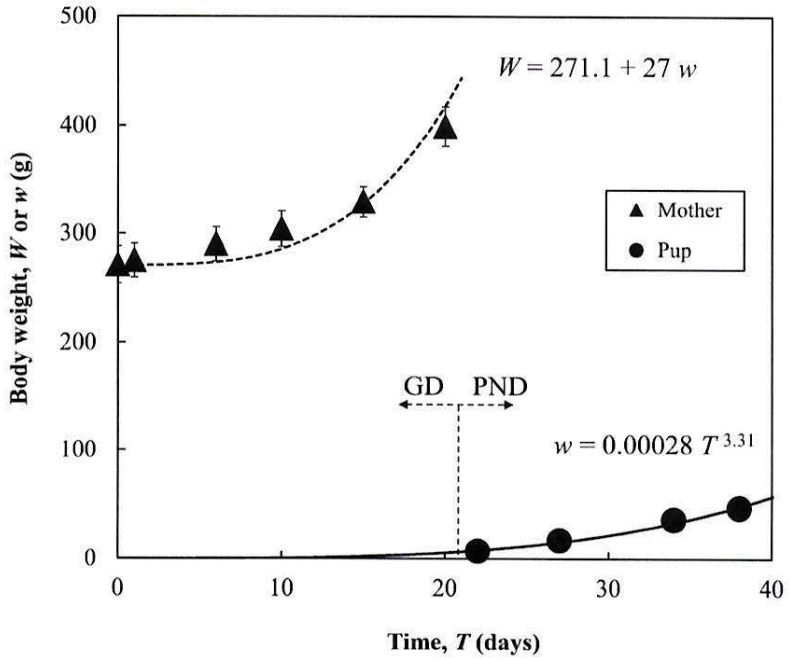

Fig. 1. The average body weight of mothers (W) exposed to 700 ppm of 1-BP up to GD20 and that of pups (w) after exposure. 1-BP: 1-bromopropane; GD: gestation day; PND: postnatal day

tion rate of bromine ion, is equal to the 1-BP uptake rate because 1-BP is decomposed quickly[11] and releases bromine ion. Under this assumption, mass balance equations of bromine ion during exposure and clearance periods respectively were as follows:

$$\frac{dx}{dt}=R-kx \tag{1}$$

$$\frac{dx}{dt}=-kx \tag{2}$$

where x is the amount of bromine ion (μg); t is time (h); R is the generation rate of bromine ion (μg/h), which corresponds to the 1-BP uptake rate; and k is the excretion rate constant (1/h). From equations (1) and (2), the bromine ion concentrations C (μg/g) during exposure and clearance respectively were obtained as follows:

$$C=\frac{R}{\rho Vk}(1-e^{-kt}) \tag{3}$$

$$C=C_0e^{-kt} \tag{4}$$

where V is the volume of the compartment (ml), ρ is the density of the compartment (g/ml), and C_0 is the initial concentration during clearance (μg/g). The excretion rate constant k is given by the biological half-life, $t_{1/2}$ (h) or $T_{1/2}$ (days).

$$k=\frac{\ln 2}{t_{1/2}\text{ (h)}}=\frac{0.693}{T_{1/2}\text{ (days)}\times 24} \tag{5}$$

Experimental Results

Fig. 1 shows the change in the average body weight of mother rats exposed to 700 ppm of 1-BP up to GD20 and that of the pups after the exposure. The time, T (on the horizontal axis), includes the GDs and PNDs. Litter sizes of exposed mothers and control mothers were 15.0 ± 2.8 and 14.9 ± 2.5 pups, respectively. The body weight of both mothers and pups increased rapidly. This tendency was also observed in the control group, and there was no significant difference between the exposure group and the control group. For the virgin female group, body weight did not change significantly (271.1 ± 17.0 g) during GD1-20.

Bromine ion concentration in the rat brain (μg/g-brain) exposed to 700 ppm of 1-BP on GDs is presented as symbols in Fig. 2. The bromine ion concentration in mother rats was lower than that in virgin rats, and the concentration in fetuses was higher than that in mothers. Fig. 3 shows changes in bromine ion concentration in pup brain for PNDs. The concentration in the gestation exposure group decreased between PND4 and PND8, whereas that in the postnatal exposure group increased from PND2 to PND4 and then decreased. This tendency was also ob-

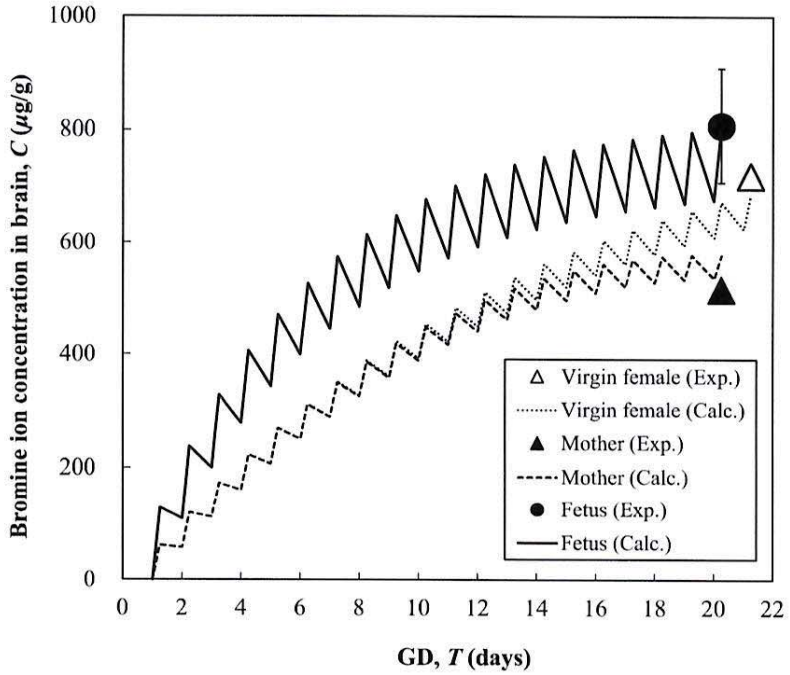

Fig. 2. Change in bromine ion concentration in rat brain exposed to 700 ppm of 1-BP on GDs. Symbols represent experimental data: ●, fetus; ▲, mother; △, virgin female. Solid, broken, and dotted lines indicate calculated lines for fetuses, mothers, and virgin females, respectively. 1-BP: 1-bromopropane; GD: gestation day

served in the exposure group, although the concentration on PND1 was lower than that on GD20 (fetus in Fig. 2). Specifically, the concentration in the exposure group was the highest just after birth, but decreased at PND1. The concentration then increased from PND1 to PND3, but decreased again with time. In the control pups, the bromine ion concentration was 11.2 ± 7.7 μg/g-brain on PND3.

The bromine ion concentration in pup stomachs with milk from the exposure group on PND1 was 830.6 ± 188.8 μg/g-stomach, which was about twice as much as that in the mother brain at GD20 (Fig. 2).

Discussion

The one-compartment model was applied to analyze the bromine ion concentration in the brains of virgin females, mothers, fetuses, and pups. Equations (3) and (4) have two parameters, the excretion rate constant k and the 1-BP uptake rate R. The excretion rate constant, k, can be easily calculated from equation (5) by using the biological half-life $T_{1/2}$ (days). In our previous work[11], $T_{1/2}$ for male rats was 4.7-15.0 days in blood and 5.0-7.5 days in urine. Therefore, $T_{1/2}$=7.0 days was used for mothers and virgin females in this study. $T_{1/2}$ in pups was 3.1 days, obtained by experimental data. Equation (4) was applied to the data from PND1 for the exposure group and from PND4 and PND8 for the gestation exposure group as shown in Fig. 3. $T_{1/2}$=3.1 days was also used for fetuses. The half-lives of between GD20 for fetuses and PND1 for the exposure group were excluded from the calculation because of the time lag due to birth.

As shown in Fig. 2, the bromine ion concentration in the brains of mothers was lower than that in the brains of virgin females. A reason for this might be that the bromine ion concentration was diluted because of increasing body weight. The average body weight of pups, w (g), was expressed using the following equation (Fig. 1):

$$w=0.00028T^{3.31} \quad (6)$$

The average body weight of mothers, W (g), was calculated as the sum of that of virgin females (ρV=271.1 g) and of pups, w, (interpolated value for GDs):

$$W=271.1+27w \quad (7)$$

where 27 is the constant, which was determined to give the best fit for the experimental data as shown in Fig. 1.

For virgin females, the uptake rate, R, of 2853 μg/h was obtained to give the best fit of equations (3) and (4) for the experimental data on GD21 in Fig. 2. Therefore, $R/\rho V=R/W$=2853/271.1=10.5 μg/(h·g) for virgin females, and $R/\rho V$=2853/(271.1 + 27w) for mother rats was used in equation (3). For fetuses, R (bromine ion uptake rate from mothers) was assumed to be proportional to body weight,

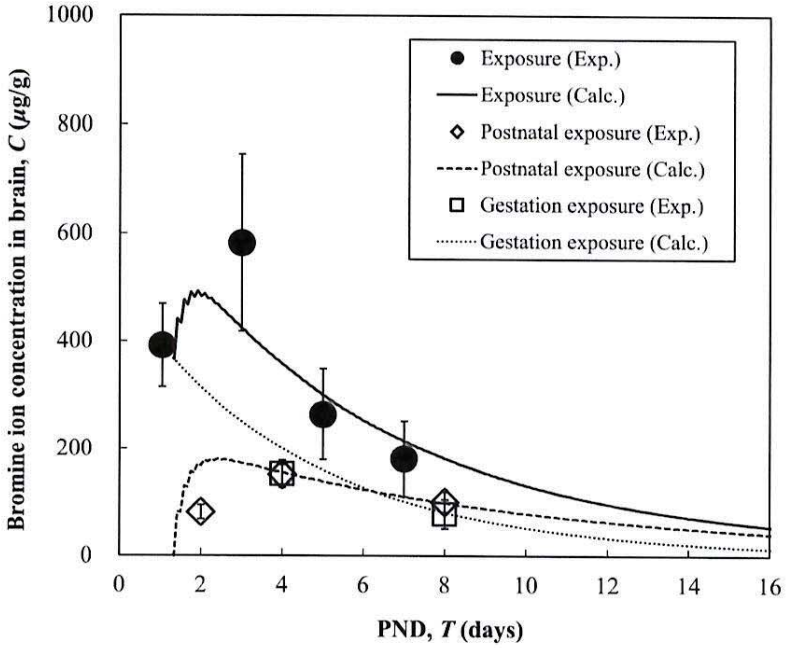

Fig. 3. Change in bromine ion concentration in pup brain during PNDs. Symbols represent experimental data: ●, exposure group (1-BP exposed pups were raised by their birth mother exposed to 1-BP); ◇, postnatal group (control pups were raised by 1-BP exposed mother); □, gestation exposure (1-BP exposed pups were raised by control mother). Solid, broken, and dotted lines indicate calculated lines for exposure, postnatal exposure, and gestation exposure groups, respectively. 1-BP: 1-bromopropane; PND: postnatal day

and $R/\rho V=R/w$=22.0 μg/(h・g) was applied, which was obtained to give the best fit for the experimental data on GD 20 in Fig. 2. On PNDs, suckling (exposure to bromine ion from milk) was assumed to occur at 2-h intervals. As shown in Fig. 3, the curve of bromine ion concentration in the brains of the postnatal exposure group is convex. In addition, on PND 1, the concentration in pup stomachs with milk was high, and the level was higher than that in the mother brain, as calculated using the one-compartment model (486.2 μg/g-brain). Therefore, we assume that the uptake rate R of pups is high at first and then decreases. In this work, R in the postnatal exposure group can be expressed by the following equation:

$$R=388e^{-0.126(t-32)} \quad (8)$$

where 32 is the initial suckling (h) and 388 and 0.126 are the constants determined experimentally. The bromine ion concentration in the exposure group was calculated as the sum of the concentrations in the gestation exposure and postnatal exposure groups. Conditions of the one-compartment model and the values of parameters obtained are listed in Table 2. Solid, broken, and dotted lines in Fig. 2 indicate calculated lines for fetuses, mothers, and virgin females, respectively. In Fig. 3, solid, broken, and dotted lines indicate calculated lines of exposure, postnatal exposure, and gestation exposure groups, respectively. The lines calculated using the proposed model could be estimated from the experimental data with acceptable precision as shown in both figures.

The calculated bromine ion uptake rates per weight, $R/\rho V$, for adults and fetuses were 10.5 and 22 μg/(h・g), respectively. This result suggests that the bromine ion easily transfers from mothers to fetuses, and the concentration in fetuses was higher than that in mothers. R in postnatal exposure group was expressed as an exponential function, and $R/\rho V$ of 55 μg/(h・g) was obtained at initial suckling time. This value was large compared to 22 μg/(h・g), the calculated value at GD20, before birth. This suggests that uptake rate of bromine ion via milk was higher than that via the placenta, and the bromine ion concentration in the exposure group could be explained as the sum of that in the gestation and postnatal exposure groups, which is shown in Fig. 3.

In summary, the results of this study suggest (1) the concentration of bromine ion in mother rats was lower than that in virgin female rats, (2) bromine ion easily transferred from mothers to fetuses and accumulated before birth, (3) bromine ion was concentrated more in milk than in the brains of the mothers, and (4) bromine ion up-

Table 2. Parameters of the one-compartment model

	Groups	$T_{1/2}$ (days)	ρV (g)	R (μg/h)	Results
GD	Virgin female	7.0	271.1	2853	Fig. 2
	Mother	7.0	271.1+27w	2853	Fig. 2
	Fetus	3.1	w	22w	Fig. 2
PND	Gestation exposure	3.1			Fig. 3
	Postnatal exposure	3.1	w	$388e^{-0.126(t-32)}$	Fig. 3
	Exposure	Gestation exposure+Postnatal exposure			Fig. 3
	Mother	7.0			Text†

†: the concentration in mother brain corresponding to PND1 (486.2 μg/g-brain), w=0.000287$^{3.31}$ by equation (6)

take rate in pups was high immediately after birth.

Acknowledgments: The authors thank Ms. Tomoko Tanaka, Kana Hayashi, Erika Ito, and Ai Kanemaru for technical help and Dr. Sumiyo Ishimatsu for her critical comments on our experiments.

Conflict of Interest: None declared.

References

1) Ichihara G. Neuro-reproductive toxicities of 1-bromopropane and 2-bromopropane. Int Arch Occup Environ Health 2005; 78: 79-96.
2) The Japan Society for Occupational Health. Recommendation of occupational exposure limits (2013-14). J Occup Health 2013; 55: 422-441.
3) Ohnishi A, Ishidao T, Kasai T, Arashidani K, Hori H. Neurotoxicity of 1-bromopropane in rats. J UOEH 1999; 21: 23-28.
4) Fueta Y, Ishidao T, Kasai T, Hori H, Arashidani K. Decreased paired-pulse inhibition in the dentate gyrus of the brain in rats exposed to 1-bromopropane vapor. J Occup Health 2000; 42: 149-151.
5) Fueta Y, Ishidao T, Arashidani K, Endo Y, Hori H. Hyperexcitability of the hippocampal CA1 and the dentate gyrus in rats subchronically exposed to a substitute for chlorofluorocarbons, 1-bromopropane vapor. J Occup Health 2002; 44: 156-165.
6) Fueta Y, Fukuda T, Ishidao T, Hori H. Electrophysiology and immunohistochemistry in the hippocampal CA1 and the dentate gyrus of rats chronically exposed to 1-bromopropane, a substitute for specific chlorofluorocarbons. Neuroscience 2004; 124: 593-603.
7) Fueta Y, Ishidao T, Ueno S, Yoshida Y, Kunugita N, Hori H. New approach to risk assessment of central neurotoxicity induced by 1-bromopropane using animal models. Neurotoxicology 2007; 28: 270-273.
8) Ueno S, Yoshida Y, Fueta Y, et al. Changes in the function of the inhibitory neurotransmitter system in the rat brain following subchronic inhalation exposure to 1-bromopropane. Neurotoxicology 2007; 28: 415-420.
9) Yoshida Y, Liu JQ, Nakano Y, et al. 1-BP inhibits NF-kB activity and Bcl-xL expression in astrocytes in vitro and reduces Bcl-xL expression in the brains of rats in vivo. Neurotoxicology 2007; 28: 381-386.
10) Yoshida Y, Nakano Y, Ueno S, et al. Effects of 1-bromopropane, a substitute for chlorofluorocarbons, on brain-derived neurotrophic factor (BDNF) expression. Int Immunopharmacol 2009; 9: 433-438.
11) Ishidao T, Kunugita N, Fueta Y, Arashidani K, Hori H. Effects of inhaled 1- bromopropane vapor on rat metabolism. Toxicol Lett 2002; 134: 237-243.
12) Ichihara G, Miller JK, Ziolkowska A, Itohara S, Takeuchi Y. Neurological disorders in three workers exposed to 1-bromopropane. J Occup Health 2002; 44: 1-7.
13) Ichihara G, Li W, Ding X, et al. A survey on exposure level, health status, and biomarkers in workers exposed to 1-bromopropane. Am J Ind Med 2004; 45: 63-75.
14) Li W, Shibata E, Zhou Z, et al. Dose-dependent neurologic abnormalities in workers exposed to 1-bromopropane. J Occup Environ Med 2010; 52: 769-777.
15) Sekiguchi S, Suda M, Zhai YL, Honma T. Effects of 1-bromopropane, 2-bromopropane, and 1,2-dichloropropane on the estrous cycle and ovulation in F344 rats. Toxicol Lett 2002; 126: 41-49.
16) Yamada T, Ichihara G, Wang H, et al. Exposure to 1-bromopropane causes ovarian dysfunction in rats. Toxicol Sci 2003; 71: 96-103.
17) Furuhashi K, Kitoh J, Tsukamura H, et al. Effects of exposure of rat dams to 1-bromopropane during pregnancy and lactation on growth and sexual maturation of their offspring. Toxicology 2006; 224: 219-228.
18) Lau C, Thibodeaux JR, Hanson RG, et al. Exposure to perfluorooctane sulfonate during pregnancy in rat and mouse. II: postnatal evaluation. Toxicological Sci 2003; 74: 382-392.
19) Hori H, Hyakudo T, Oyabu T, Ishimatsu S, Yamato H, Tanaka I. Effects of inhaled methyl bromide gas on the metabolic system and kinetics of bromine ion in rats. J UOEH 2002; 24: 151-160.

E-mail addresses;

yukiko@med.uoeh-u.ac.jp (Yukiko FUETA)

yukos@nihs.go.jp (Yuko SEKINO)

syoshida@ens.tut.ac.jp (Sachiko YOSHIDA)

kanda@nihs.go.jp (Yasunari KANKDA)

susumu@med.uoeh-u.ac.jp (Susumu UENO)

Corresponding author

Susumu UENO

Department of Occupational Toxicology, Institute of Industrial Ecological Sciences, University of Occupational and Environmental Health, Japan

1-1 Iseigaoka, Yahatanishi-ku, Kitakyushu 807-8555, Japan.

Tel: +81-93-691-7404

Fax: +81-93-692-4790

E-mail: susumu@med.uoeh-u.ac.jp

Abstract

Prenatal valproic acid (VPA) exposure is a well-known animal model of autism spectrum disorder (ASD) that produces alterations in embryonic and adult neurogenesis as well as adolescent/adulthood neurobehavioral phenotypes. However, the effects of prenatal VPA exposure on neural network excitability, especially during the synaptogenic period around eye opening, are not fully understood. In this study, we orally administered VPA (300 mg/kg) to pregnant Wistar rats on gestation day 15 and subsequently performed field potential recording in the CA1 area of hippocampal slices obtained from control (saline-exposed) and VPA-exposed rat pups between postnatal day (PND) 13 and PND18. In control slices, we observed an abrupt enhancement of stimulation-dependent responses including population spike (PS) amplitudes and field excitatory postsynaptic potential (fEPSP) slopes at PND16, which coincided with the average day of eye opening. In contrast, VPA-exposed pups exhibited delayed eye opening (PND17) and gradual rather than abrupt increases in PS amplitudes and fEPSP slopes over the duration of the synaptogenic period. We next investigated the involvement of ambient GABA in PS generation using bicuculline methiodide (BMI), a γ-aminobutyric acid type A ($GABA_A$) receptor antagonist. In control slices, BMI enhanced PS amplitudes during PND14–15 (before eye opening) and had little effect

thereafter during PND16–17; a subsequent regression model analysis of BMI ratios (the ratio of PS amplitudes in the presence and absence of BMI) indicated a possible developmental change between these periods. In contrast, almost identical regression models were obtained for BMI ratios during PND14–15 and PND16–17 in the VPA-exposed group, indicating the absence of a developmental change. Our results suggest that prenatal VPA exposure accelerates the development of hippocampal excitability before eye opening. Moreover, our experimental model can be used as a novel approach for the evaluation of developmental neurotoxicity.

Key words:

developmental neurotoxicity; valproic acid; prenatal exposure; hippocampus; slice preparation; electrophysiology

1. Introduction

The impact of exogenous chemical substances on childhood neural development, also known as developmental neurotoxicity, is an important social issue (Andersen et al., 2000; Grandjean and Landrigan, 2006). Valproic acid (VPA) is an antiepileptic drug and mood stabilizer that has been reported to increase the risk of autism spectrum disorders (ASD) in children when women take VPA during early pregnancy (Chomiak et al., 2013). Similarly, rodent models of ASD have been established using prenatal exposure to VPA; in VPA exposure-based models, offspring exhibit autism-like behaviors including impaired social interactions and repetitive behaviors (Markram et al., 2008; Rodier et al., 1997; Roullet et al., 2013; Schneider and Przewlocki, 2005). In addition to neurobehavioral phenotypes, ASD model animals exhibit alterations in embryonic and adult neurogenesis (Juliandi et al., 2015). However, it is not well known whether prenatal exposure to VPA also affects neurogenesis in developmental stages occurring prior to adulthood, especially during the synaptogenic period.

Neural activity is a critical regulator of neural network development. It was recently demonstrated that spine density is remarkably increased in the hippocampal CA1 area of mice between postnatal day (PND) 11 and PND21, i.e. during the synaptogenic period (Johnson-Venkatesh et al., 2015). Interestingly, when intrinsic neural activity was

suppressed by overexpression of Kir2.1, an inwardly rectifying K^+ channel, increases in spine density during the synaptogenic period were abolished. Thus, neural network activity in the hippocampal CA1 area is necessary for healthy neural development during the synaptogenic period including around eye opening.

Chloride conductance due to ambient concentrations of GABA (γ-aminobutyric acid) also plays a role in regulating neural network excitability during postnatal neural development (Cellot and Cherubini, 2013; Kilb et al., 2013). Ambient GABA originates from the spillover of neurotransmitter escaping the synaptic cleft and from astrocytes via a non-vesicular Ca^{2+}-independent process and mediates tonic inhibition via extrasynaptic $GABA_A$ receptors. However, there is little evidence demonstrating effects of prenatal exposure to toxicants including VPA on ambient GABA-mediated inhibition of neural network excitability.

In the present study, we used a model of prenatal VPA exposure and evaluated effects on neural network activity in the hippocampal CA1 area during the synaptogenic period using hippocampal slices from PND13–18 rat pups. We not only observed the ability of prenatal VPA exposure to abolish development-associated enhancements in stimulation-dependent neural responses, but also confirmed the ability of prenatal exposure to influence ambient GABA-mediated inhibition even prior to eye opening.

2. Material and Methods

2.1 Animals

Adult Wistar/ST rats were purchased from Japan SLC *Inc*. (Japan). Rats were housed in plastic cages on paper chip bedding (ALPHA-dri, Shepherd Specialty Papers, USA) and maintained on a 12-h light/dark cycle (light period: 07:00–19:00) in a room with controlled temperature (23 ± 1°C) and relative humidity (50 ± 15%). Animals were given free access to food (CE2, CLEA Japan Inc., Japan) and filtered water (TCW-PPS filter, Advantech Co., LTD., Japan) dispensed in glass water supply bottles.

The proestrus stage was verified with an impedance checker (MK-10B, Muromachi Kikai Co., Ltd., Japan). When the observed impedance was > 3 kΩ female rats were provided with a male rat for mating. The presence of a vaginal plug or sperm in the vaginal smear the following morning confirmed coition, and it was regarded as gestation day (GD) “zero” (Fig. 1). Pregnant rats were randomly divided into two groups: a control group and a VPA exposure group.

VPA was purchased from Wako Pure Chemical Industries, Ltd. (Japan), dissolved in physiological saline (Otsuka Pharmaceutical Co., Ltd, Japan), and orally administered to dams (300 mg/kg) on GD15 under 5% isoflurane gas anesthesia (Pfizer Japan Inc., Japan).

All dams gave birth on GD21, and the date of birth was defined as PND0. If there were more than 10 pups in a litter, the litter size was adjusted to 10 pups on PND1. Litters of less than 10 pups were not adjusted. All pups were housed with their dams during the lactation period. Rat pup body weights were measured on PND1, PND7, PND14, and PND21. The day of eye opening was determined by checking the eyes of pups at 14:00 on each day from PND15–18.

For the electrophysiological study, the control group included pups from 16 control dams and the VPA-exposed group included pups from 17 VPA-exposed dams. All studies were approved by the Ethics Committee on Animal Care and Experimentation and performed in accordance with the guidelines of the University of Occupational and Environmental Health, Japan.

2.2 Slice preparation and recordings

Hippocampal slices (600 μm thickness) were prepared from male pups on each postnatal day between PND13–18 as previously described (Fueta et al., 2004; Fueta et al., 2002). Slices were perfused with artificial cerebrospinal fluid (ACSF) containing 124 mM NaCl, 2 mM KCl, 2 mM $MgSO_4$, 2 mM $CaCl_2$, 1.25 mM KH_2PO_4, 26 mM $NaHCO_3$, and 10 mM glucose; saturated with an O_2 95%/CO_2 5% gas mixture; and

stored in a thermostatic bath (27.6°C). The perfusion rate of ACSF was 1 ml/min for all experiments.

Population spikes (PSs) and field excitatory synaptic potentials (fEPSPs) were simultaneously recorded from the CA1 area of hippocampal slices using glass microelectrodes (Fig. 2A). For slices obtained during the period from PND13–15, PSs were recorded from the area between the pyramidal cell layer and the alveus. The recording positions for PSs and fEPSPs were similar between the control and VPA-exposed groups. Bipolar stimulation electrodes made of stainless wires (50 μm in diameter) were placed on Shaffer collateral/commissural fibers at a distance of about 250 μm from the fEPSP recording electrodes. Stimulation-response relationships were observed with stimulation intensities from 10–600 μA. The stimulation interval was 2 min in order to avoid the measurement of overlapping stimulation effects.

Between PND14–17, experiments evaluated the effects of bicuculline methiodide (BMI, Tocris Bioscience, U.K.), a $GABA_A$ receptor antagonist, on the generation of PSs. Average PS amplitudes in response to 600 μA stimulation were recorded in triplicate (with 2-min intervals) in the absence and presence of BMI; after PS measurements in the absence of BMI, slices were perfused with ACSF containing BMI (1 μM) for 10 min and subsequently tested. A total of 3–4 slices per rat pup were tested.

2.3 Distribution analysis

Histogram distribution and nonlinear regression analyses of BMI ratios (PS amplitude in the presence of BMI divided by that in the absence of BMI) were conducted using GraphPad Prism software (GraphPad Software, Inc., USA).

2.4 Statistical analysis

Litter sizes and sex ratios as well as pup body weights and the day of eye opening are expressed as the mean ± standard deviation (SD). Electrophysiological results are expressed as the mean ± standard error of mean (SEM). Statistical differences between the control and VPA-exposed groups were determined using two-sided Student's *t*-tests or Mann-Whitney U tests at a significance level of $P < 0.05$.

3. Results

For the purpose of our study, the time of eye opening in our rat models was needed to confirm. In consequence, the average day of eye opening was significantly delayed in the VPA-exposed group compared to the control group ($P<0.01$, Table 1). We also examined general toxicity induced by one-time prenatal VPA exposure at GD15, and found that there were no significant differences between the control and VPA-exposed groups in terms of litter size, litter sex ratio, or changes in pup body weight. Moreover, the number of pups that died before experimentation or weaning was not significantly different between groups (control group, 2 of 206 pups; VPA-exposed group, 4 of 195 pups).

Next, to investigate neural network excitability during the synaptogenic period, we studied stimulation-response (S/R) relationships for fEPSP slopes and PS amplitudes using hippocampal slice preparations, in which the cytoarchitecture and synaptic circuits of the hippocampus are largely retained. S/R relationships exhibited two different stages; similar degrees of stimulation-dependent responses were observed in control pups between PND13–15. However, responses (fEPSP slopes and PS amplitudes) were suddenly augmented on PND16, which seemed to correspond with eye opening. Responses were maintained at an enhanced level for fEPSP slopes and

slightly enhanced for PS amplitudes between PND17–18 (Fig. 2B, C).

In contrast, a gradual enhancement of S/R relationships was observed between PND13–18 in the VPA-exposed group, and did appear to correspond with eye opening. Therefore, we reanalyzed fEPSP slopes and PS amplitudes in response to a stimulation intensity of 600 μA, which evoked the maximal responses. PS amplitudes obtained from the control group showed an abrupt increase between PND15–16, whereas those from the VPA-exposed group again demonstrated a gradual increase over the period examined, with significant differences at PND14 and PND15 compared to the control group. A similar but smaller developmental change was observed in the fEPSP slope, with a significant difference between the control and VPA-exposed groups on PND15 (Fig. 3).

Next we investigated the effect of BMI on PS generation in order to elucidate the role of ambient GABA in postnatal PS generation. Fig. 4 shows the effect of BMI on PS amplitudes in the control group before eye opening (PND14–15) and after eye opening (PND16–17). PS amplitudes were enhanced in the presence of BMI during PND14–15 (Fig. 4A, left), but this enhancement was attenuated during PND16–17 (Fig. 4B, left). The mean BMI ratios (ratio of the PS amplitude in the presence of BMI to that in the absence of BMI) were 1.80 ± 0.17 (n = 13) for PND14–15 and 1.14 ± 0.04 (n = 10)

for PND16–17. Histograms of BMI ratios (Figs. 4A and 4B, right) and nonlinear regression analyses revealed a clear developmental change in the probability distribution of BMI ratios for PS amplitudes (Fig. 6, left).

In contrast, for the VPA-exposed group, PS amplitudes generated in the presence of BMI showed small or little increases during both the PND14–15 and PND16–17 periods (Figs. 5A and 5B, left). The mean BMI ratios were 1.34 ± 0.14 (n = 17) for PND14–15 and 1.14 ± 0.05 (n = 17) for PND16–17. Moreover, histograms of BMI ratios and nonlinear regression analyses (Figs. 5A and 5B, right) were almost identical between the PND14–15 and PND16–17 periods, suggesting attenuation of the developmental change observed in the control group (Fig. 6, right). We also investigated the responses to BMI for fEPSP slopes, but minimal (non-significant) BMI responses and alterations in developmental change were observed.

4. Discussion

In this study, we investigated the effect of prenatal VPA exposure on the development of neural network activity in the hippocampal CA1 area during the synaptogenic period, including during the period of eye opening. A single dose of VPA (300 mg/kg) was orally administered to dams on GD15 and was not noted to affect dam maternal behavior or fetal/neonatal mortality. In animal models of ASD, VPA is often administered repeatedly or earlier than GD11.5 prior to closure of the neural tube (Rodier et al., 1997). Therefore, the most effective period for observing the effects of prenatal VPA exposure as it relates to ASD may be earlier than GD15.

Brain slice preparation is a well-known laboratory technique for electrophysiology and pharmacology research. Since local neuronal circuits remain intact in brain slices, this neurophysiological preparation is useful for studying neurotoxicity (Fountain et al., 1992) as well as the specific effects of neurotoxic agents on synaptic transmission and plasticity (Varela et al., 2012; Wiegand and Altmann, 1994). The electrophysiological strategy used in the present work has been previously implemented to study the effects of prenatal/perinatal ethanol exposure (Puglia and Valenzuela, 2010), lead (Carpenter et al., 2002; Sui et al., 2000), polychlorinated biphenyl exposure (Altmann et al., 1998; Carpenter et al., 2002; Kim and Pessah, 2011), and toluene exposure (Chen et al., 2011).

Thus, we deemed the present model to be useful for evaluating excitatory/inhibitory function and developmental neurotoxicity after VPA exposure.

Our first main finding was that stimulation-dependent responses for fEPSPs and PSs in the hippocampal CA1 area showed two different periods of development in normal pups; one from PND13–15 before eye opening on PND16, and another after eye opening from PND16–18. S/R relationships for neural excitability in the CA1 area exhibited drastic enhancements after eye opening. Alternatively, we did not observe clear discrimination between stimulation-dependent responses before and after eye opening in the VPA-exposed group; enhancements in stimulation-dependent CA1 excitability were observed on PND14 and/or PND15 in the VPA-exposed group compared to the control group, and gradual changes were observed in the subsequent postnatal days. In other words, prenatal VPA exposure appeared to accelerate developmental changes in neural excitability that otherwise appeared in association with eye opening in healthy pups.

Ambient GABA is a critical factor that regulates neural network excitability. Therefore, we also investigated the involvement of ambient GABA in PS generation using BMI, a $GABA_A$ receptor antagonist. On PND14 and PND15 before eye opening, PS amplitudes evoked in the presence of BMI were greater than those in the control

condition, suggesting a possible role for PS inhibition by ambient GABA. On PND 16 and PND17 on or after eye opening, BMI had little effect on PS amplitudes. These results indicated that ambient GABA was involved in suppressing neural excitability in the CA1 area during neural development prior to eye opening. The centering of this developmental change around the event of eye opening is consistent with a previous report that demonstrated notable increases in spine density on PND15 (Johnson-Venkatesh et al., 2015).

In contrast, BMI had little effect on PS generation before or after eye opening in the VPA-exposed group. Indeed, nonlinear regression models of distribution histograms obtained during PND14–15 and PND16–17 were virtually identical. These results suggest that prenatal exposure to VPA may eliminate ambient GABA suppression of neural excitability prior to eye opening, and are consistent with the observation of enhanced stimulation-dependent responses at PND14 and PND15 in the VPA-exposed group. Accordingly, prenatal exposure to VPA may accelerate neural development in CA1 area during the synaptogenic period.

Ambient GABA-mediated tonic inhibition in hippocampal neurons is synergistically modulated by two GABA transporters (GATs): GAT-1 located on presynaptic membranes and GAT-3 on astrocytes (Egawa and Fukuda, 2013; Kersante et al., 2013).

GAT-1 is predominantly responsible for GABA reuptake under resting conditions; alternatively, GAT-3 plays an important role in controlling hippocampal cell excitability during neural activation (Kersante et al., 2013). Therefore, our findings raise the question of whether developmental changes in evoked PS responses to BMI were related to alterations in the expression and/or function of GATs in the CA1 area during development. Further investigations are in progress to address this issue.

Among several hypothetical mechanisms underlying ASD, the disruption of excitation/inhibition (E/I) balance in neuronal circuits has been proposed as a unifying explanation for the complexity and diversity of ASD presentations arising from genetic (Gkogkas et al., 2013; Gogolla et al., 2009; Rubenstein, 2010; Rubenstein and Merzenich, 2003) and environmental factors (Rubenstein and Merzenich, 2003). Although the precise mechanisms of altered E/I balance after prenatal exposure to VPA have not been fully elucidated, this effect has been replicated in several rodent studies. Rinaldi et al. showed that prenatal injection of VPA (500 mg/kg, intraperitoneally) increased N-methyl-D-aspartate (NMDA) receptor subunit protein expression in the whole brains of pups and enhanced NMDA receptor-mediated synaptic currents in neocortical slices obtained from pups during PND12–16 (Rinaldi et al., 2007). These authors further reported that prenatal VPA exposure induced local circuits

hyperconnectivity and enhancements in both excitatory and inhibitory systems in the sensory cortex (Rinaldi et al., 2008). Banerjee et al. reported that a single intraperitoneal injection of VPA (600 mg/kg) at GD11.5 impaired postnatal GABAergic synaptic transmission using slice preparations of the auditory cortex from PND23–45 offspring (Banerjee et al., 2013).

To the best of our knowledge, this is the first report to describe a possible role for GABA-mediated inhibition in the development of evoked PSs during the synaptogenic period around eye opening. Moreover, our data suggest that prenatal exposure to VPA and potentially other developmental neurotoxicants at specific points of the gestation period can accelerate this developmental change. Changes in PS amplitudes evoked from hippocampal slices during prenatal development, especially in the presence of BMI, may be useful as an index for the normal development of neural circuits; to this end, our assay may have utility for screening other candidate neurodevelopmental toxicants. Studies with other known toxicants including organometallic compounds and pesticides are in progress to determine whether similar developmental alterations can be observed using the current experimental approach.

5. Conclusions

In summary, we report that one-time prenatal exposure to VPA at GD 15 produced enhancements in stimulation-dependent responses for fEPSP slopes and PS amplitudes in the CA1 area of offspring, and moreover altered offspring PS amplitude responses to BMI. Taken together, prenatal VPA exposure may transiently alter E/I balance, resulting in the acceleration of neural development before eye opening. This effect corresponds with the hypothetical mechanisms underlying ASD; that is, the disruption of E/I balance in developing brain circuits. Although further investigations are required, our results provide an alternative approach for the evaluation of developmental neurotoxicity.

Funding information

This study was supported by Health and Labor Sciences Research Grants of the Ministry of Health, Labour and Welfare in Japan.

Conflict of interest statement

The authors declare that there is no conflict of interest.

Acknowledgement

The authors would like to thank Kaoru Sato, Seiichi Ishida, and Daiju Yamazaki for helpful discussion.

Table 1. Litter sizes and sex ratios as well as pup weight gain and the day of eye opening for the control and VPA-exposed groups.

	control		VPA-exposed	
litter size of dams	12.0 ± 2.0	(21)	13.0 ± 3.0	(20)
sex ratio of pups (male/female, %)	48.5 ± 0.1	(21)	49.5 ± 0.1	(20)
male pup weight (g)				
PND1	6.0 ± 0.6	(55)	5.7 ± 0.4	(53)
PND7	14.9 ± 1.6	(54)	14.1 ± 1.3	(47)
PND14	30.1 ± 1.9	(47)	28.6 ± 2.2	(45)
PND21	50.2 ± 4.3	(20)	46.9 ± 3.7	(23)
Day of eye opening	16.5 ± 0.6	(67)	17.3 ± 0.7**	(77)

Data represent the mean ± standard deviation. Numbers in parentheses are total numbers of dams/pups examined. **P<0.01, compared to the control. Abbreviations: PND, postnatal day; VPA, valproic acid.

References

Altmann, L., Lilienthal, H., Hany, J., Wiegand, H., 1998. Inhibition of long-term potentiation in developing rat visual cortex but not hippocampus by in utero exposure to polychlorinated biphenyls. Brain Res. Dev. Brain Res. 110, 257-260.

Andersen, H.R., Nielsen, J.B., Grandjean, P., 2000. Toxicologic evidence of developmental neurotoxicity of environmental chemicals. Toxicology 144, 121–127.

Banerjee, A., Garcia-Oscos, F., Roychowdhury, S., Galindo, L.C., Hall, S., Kilgard, M.P., Atzori, M., 2013. Impairment of cortical GABAergic synaptic transmission in an environmental rat model of autism. Int. J. Neuropsychopharmacol. 16, 1309–1318.

Carpenter, D.O., Hussain, R.J., Berger, D.F., Lombardo, J.P., Park, H.Y., 2002. Electrophysiologic and behavioral effects of perinatal and acute exposure of rats to lead and polychlorinated biphenyls. Environ. Health Perspect. 110 Suppl 3, 377–386.

Cellot, G., Cherubini, E., 2013. Functional role of ambient GABA in refining neuronal circuits early in postnatal development. Front. Neural Circuits 7, 136.

Chen, H.H., Lin, Y.R., Chan, M.H., 2011. Toluene exposure during brain growth spurt and adolescence produces differential effects on N-methyl-D-aspartate

receptor-mediated currents in rat hippocampus. Toxicol. Lett. 205, 336–340.

Chomiak, T., Turner, N., Hu, B., 2013. What We Have Learned about Autism Spectrum Disorder from Valproic Acid. Patholog. Res. Int. 2013, 712758.

Egawa, K., Fukuda, A., 2013. Pathophysiological power of improper tonic GABA(A) conductances in mature and immature models. Front. Neural Circuits 7, 170.

Fountain, S.B., Ting, Y.L., Teyler, T.J., 1992. The in vitro hippocampal slice preparation as a screen for neurotoxicity. Toxicol. In Vitro 6, 77–87.

Fueta, Y., Fukuda, T., Ishidao, T., Hori, H., 2004. Electrophysiology and immunohistochemistry in the hippocampal ca1 and the dentate gyrus of rats chronically exposed to 1-bromopropane, a substitute for specific chlorofluorocarbons. Neuroscience 124, 593–603.

Fueta, Y., Ishidao, T., Arashidani, K., Endo, Y., Hori, H., 2002. Hyperexcitability of the Hippocampal CA1 and the Dentate Gyrus in Rats Subchronically Exposed to a Substitute for Chlorofluorocarbons, 1-Bromopropane Vapor. J. Occup. Health 44, 156–165.

Gkogkas, C.G., Khoutorsky, A., Ran, I., Rampakakis, E., Nevarko, T., Weatherill, D.B., Vasuta, C., Yee, S., Truitt, M., Dallaire, P., Major, F., Lasko, P., Ruggero, D., Nader, K., Lacaille, J.C., Sonenberg, N., 2013. Autism-related deficits via dysregulated

eIF4E-dependent translational control. Nature 493, 371–377.

Gogolla, N., Leblanc, J.J., Quast, K.B., Sudhof, T.C., Fagiolini, M., Hensch, T.K., 2009. Common circuit defect of excitatory-inhibitory balance in mouse models of autism. J. Neurodev. Disord. 1, 172–181.

Grandjean, P., Landrigan, P.J., 2006. Developmental neurotoxicity of industrial chemicals. Lancet 368, 2167–2178.

Johnson-Venkatesh, E.M., Khan, M.N., Murphy, G.G., Sutton, M.A., Umemori, H., 2015. Excitability governs neural development in a hippocampal region-specific manner. Development 142, 3879–3891.

Juliandi, B., Tanemura, K., Igarashi, K., Tominaga, T., Furukawa, Y., Otsuka, M., Moriyama, N., Ikegami, D., Abematsu, M., Sanosaka, T., Tsujimura, K., Narita, M., Kanno, J., Nakashima, K., 2015. Reduced Adult Hippocampal Neurogenesis and Cognitive Impairments following Prenatal Treatment of the Antiepileptic Drug Valproic Acid. Stem Cell Reports 5, 996–1009.

Kersante, F., Rowley, S.C., Pavlov, I., Gutierrez-Mecinas, M., Semyanov, A., Reul, J.M., Walker, M.C., Linthorst, A.C., 2013. A functional role for both -aminobutyric acid (GABA) transporter-1 and GABA transporter-3 in the modulation of extracellular GABA and GABAergic tonic conductances in the rat hippocampus. J. Physiol. 591,

2429–2441.

Kilb, W., Kirischuk, S., Luhmann, H.J., 2013. Role of tonic GABAergic currents during pre- and early postnatal rodent development. Front. Neural Circuits 7, 139.

Kim, K.H., Pessah, I.N., 2011. Perinatal exposure to environmental polychlorinated biphenyls sensitizes hippocampus to excitotoxicity ex vivo. Neurotoxicology 32, 981–985.

Markram, K., Rinaldi, T., La Mendola, D., Sandi, C., Markram, H., 2008. Abnormal fear conditioning and amygdala processing in an animal model of autism. Neuropsychopharmacology 33, 901–912.

Puglia, M.P., Valenzuela, C.F., 2010. Repeated third trimester-equivalent ethanol exposure inhibits long-term potentiation in the hippocampal CA1 region of neonatal rats. Alcohol 44, 283–290.

Rinaldi, T., Kulangara, K., Antoniello, K., Markram, H., 2007. Elevated NMDA receptor levels and enhanced postsynaptic long-term potentiation induced by prenatal exposure to valproic acid. Proc. Natl. Acad. Sci. U. S. A. 104, 13501–13506.

Rinaldi, T., Perrodin, C., Markram, H., 2008. Hyper-connectivity and hyper-plasticity in the medial prefrontal cortex in the valproic Acid animal model of autism. Front.

Neural Circuits 2, 4.

Rodier, P.M., Ingram, J.L., Tisdale, B., Croog, V.J., 1997. Linking etiologies in humans and animal models: studies of autism. Reprod. Toxicol. 11, 417–422.

Roullet, F.I., Lai, J.K., Foster, J.A., 2013. In utero exposure to valproic acid and autism--a current review of clinical and animal studies. Neurotoxicol. Teratol. 36, 47–56.

Rubenstein, J.L., 2010. Three hypotheses for developmental defects that may underlie some forms of autism spectrum disorder. Curr. Opin. Neurol. 23, 118–123.

Rubenstein, J.L., Merzenich, M.M., 2003. Model of autism: increased ratio of excitation/inhibition in key neural systems. Genes Brain. Behav. 2, 255–267.

Schneider, T., Przewlocki, R., 2005. Behavioral alterations in rats prenatally exposed to valproic acid: animal model of autism. Neuropsychopharmacology 30, 80–89.

Sui, L., Ge, S.Y., Ruan, D.Y., Chen, J.T., Xu, Y.Z., Wang, M., 2000. Age-related impairment of long-term depression in area CA1 and dentate gyrus of rat hippocampus following developmental lead exposure in vitro. Neurotoxicol. Teratol. 22, 381–387.

Varela, C., Llano, D.A., Theyel, B.B., 2012. An Introduction to In Vitro Slice Approaches for the Study of Neuronal Circuitry, in: Fellin, T., Halassa, M. (Eds.),

Neuronal Network Analysis: Concepts and Experimental Approaches. Humana Press, Totowa, pp. 103–125.

Wiegand, H., Altmann, L., 1994. Neurophysiological aspects of hippocampal neurotoxicity. Neurotoxicology 15, 451–458

Figure legends

Figure 1. Scheme of the experimental design.

Figure 2. Stimulation/response (S/R) relationships for population spike (PS) amplitudes and field excitatory postsynaptic potential (fEPSP) slopes recorded from the hippocampal CA1 area of rats that were prenatally exposed to valproic acid (VPA). (A) Illustration depicting the procedure of fEPSP and PS recordings from CA1. Responses were evoked with a stimulating electrode placed in the stratum radiatum. Thick lines on the left traces indicate how measurements of fEPSP slopes and PS amplitudes were taken. (B, C) In control rats (left graphs), the S/R relationships for both fEPSP slopes and PS amplitudes were enhanced between PND15–16. Data were collected from 14–19 slices obtained from pups of 4–5 different litters. In VPA-exposed rats (right graphs), these relationships were gradually enhanced between PND13–18. Data were gathered from 10–17 slices obtained from pups of 5–6 different litters. The x-axis is stimulation intensity and the y-axis is size of the fEPSP slope or PS amplitude. Data represent the mean ± standard error of the mean.

Figure 3. Developmental changes in population spike (PS) amplitudes and field

excitatory postsynaptic potentials (fEPSPs) slopes in the control and valproic acid (VPA)-exposed groups. One-time prenatal exposure to VPA (300 mg/kg) led to postnatal increases in PS amplitude and fEPSP slope during PND14–15 and PND15, respectively. There were no between-group differences in excitability between PND16–18. The stimulation intensity was 600 μA. * indicates $P < 0.05$ using a Student's *t*-test. ++ indicates $P < 0.01$ using a Mann-Whitney U test.

Figure 4. Development-associated changes in population spike (PS) amplitude responses to BMI in the control group. (A) At PND14–15, application of the $GABA_A$ receptor antagonist BMI to hippocampal slices during recording remarkably increased PS amplitudes; the mean BMI ratio was 1.80 (95% confidence interval = 1.44–2.16). (B) Increased PS amplitudes in response to BMI application were not observed at PND16–17; the mean ratio was 1.14 (95% confidence interval = 1.04–1.24).

Figure 5. Development-associated changes in population spike (PS) amplitude responses to BMI in the valproic acid (VPA)-exposed group. Hippocampal slices from the VPA-exposed group were virtually insensitive to BMI during both the PND14–15 (A) and PND16–17 (B) periods; the mean BMI ratios were 1.34 (95% confidence

interval = 1.04–1.64) and 1.14 (95% confidence interval = 1.04–1.25), respectively.

Figure 6. Developmental alterations in nonlinear regression models of BMI ratios for population spike (PS) responses. Data from right figure panels of 4 and 5 were re-plotted and summarized for the control (left panel) and VPA-exposed groups (right panel).

Fig.1

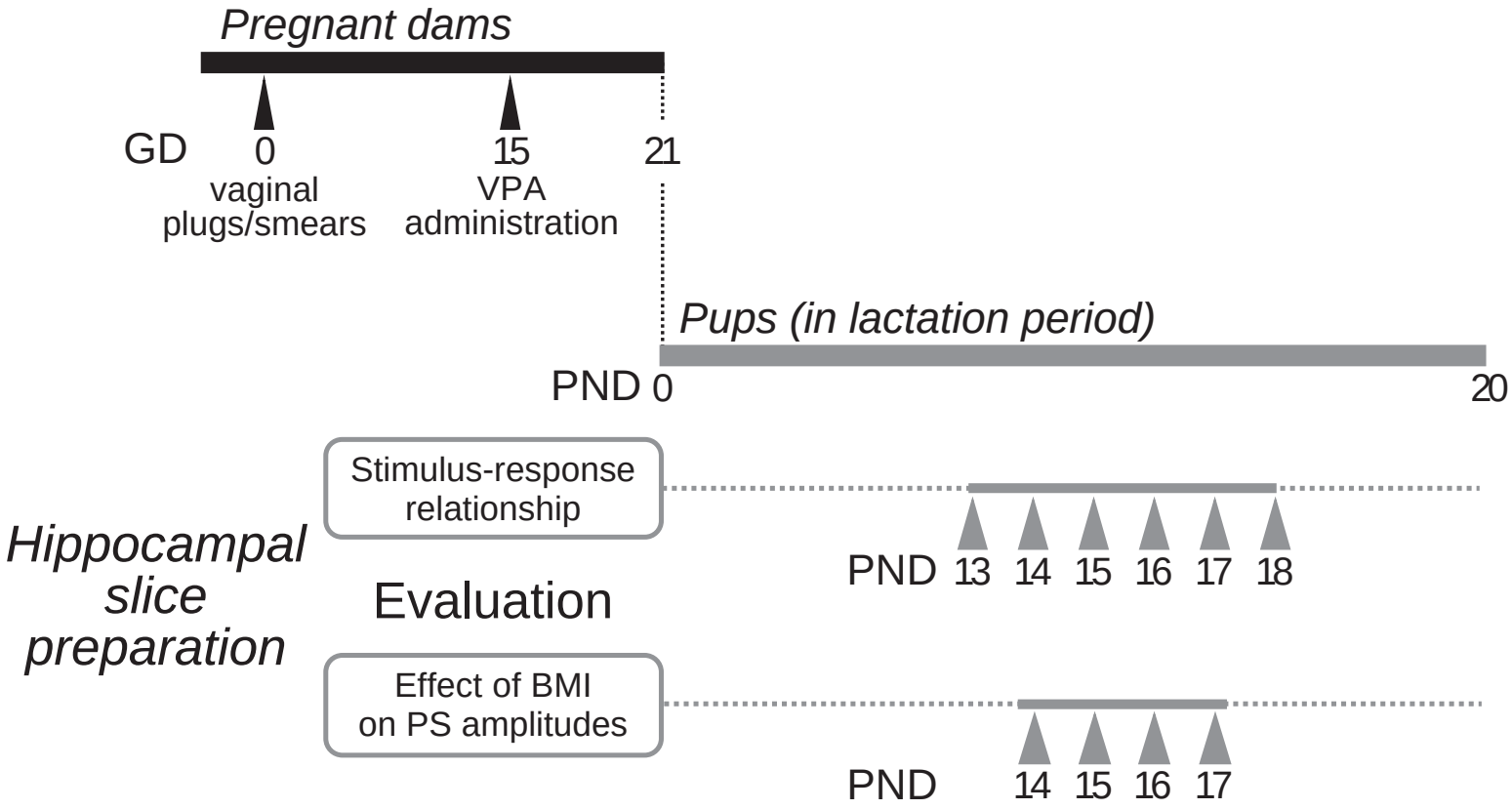
Pregnant dams
GD
0
vaginal plugs/smears
15
VPA administration
21
Pups (in lactation period)
PND 0
20
Hippocampal slice preparation
Stimulus-response relationship
PND 13 14 15 16 17 18
Evaluation
Effect of BMI on PS amplitudes
PND 14 15 16 17

Fig.2

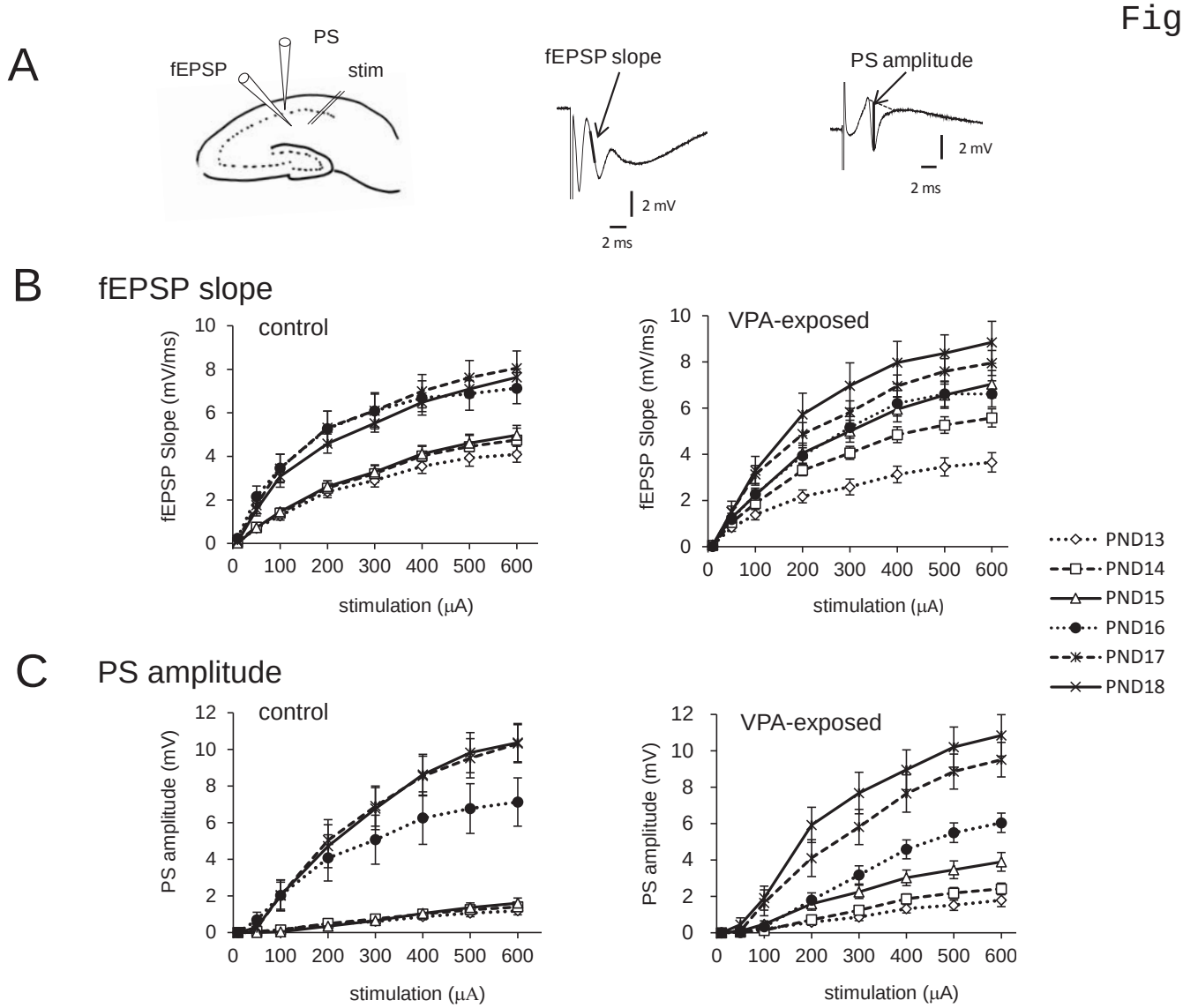
A
PS
fEPSP
stim
fEPSP slope
2 mV
2 ms
PS amplitude
2 mV
2 ms
B
fEPSP slope
control
VPA-exposed
fEPSP Slope (mV/ms)
stimulation (μA)
PND13
PND14
PND15
PND16
PND17
PND18
C
PS amplitude
control
VPA-exposed
PS amplitude (mV)
stimulation (μA)

Fig.3

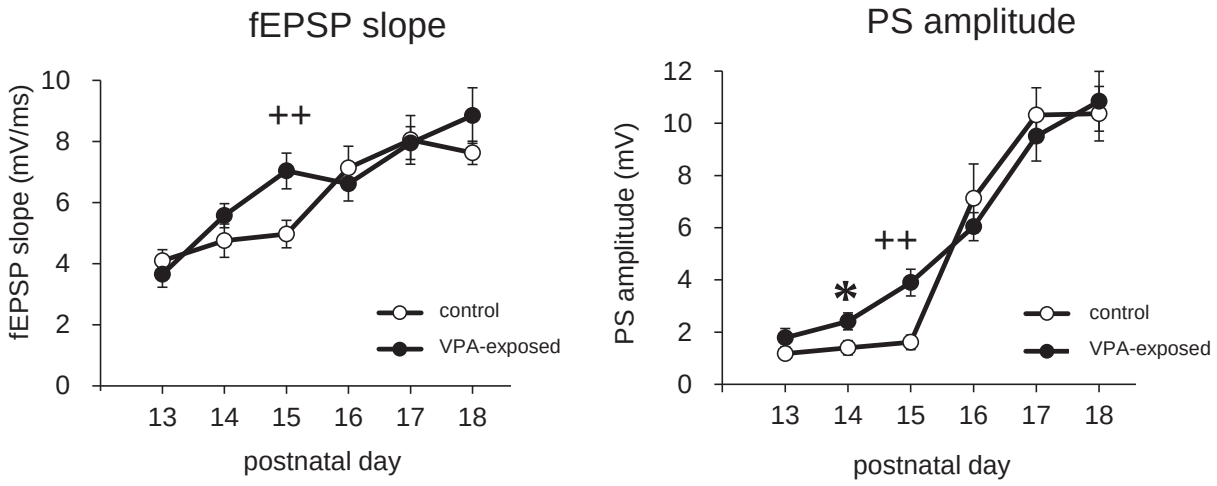
fEPSP slope
fEPSP slope (mV/ms)
0
2
4
6
8
10
++
control
VPA-exposed
13
14
15
16
17
18
postnatal day
PS amplitude
PS amplitude (mV)
0
2
4
6
8
10
12
*
++
control
VPA-exposed
13
14
15
16
17
18
postnatal day

Fig.4

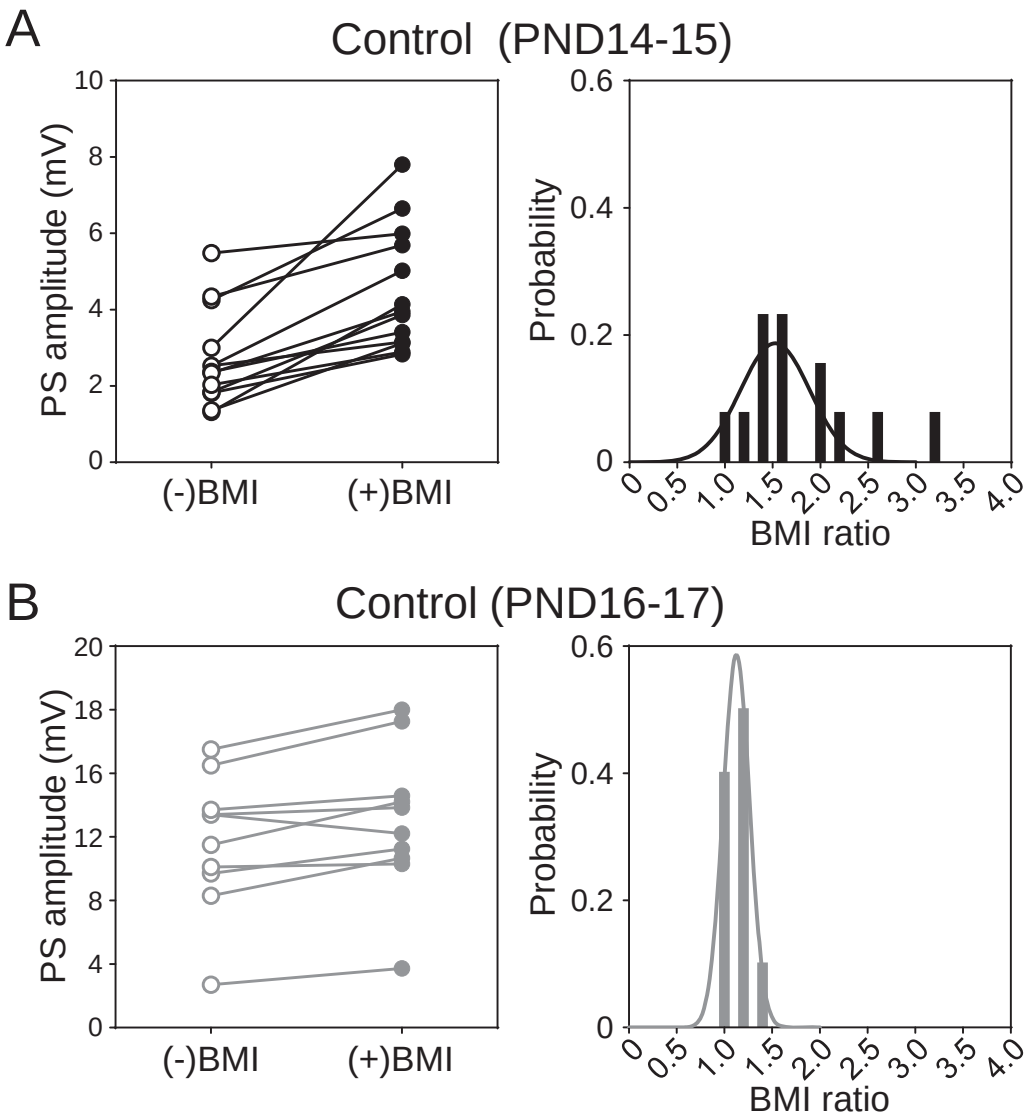
A
Control (PND14-15)
PS amplitude (mV)
10
8
6
4
2
0
(-)BMI
(+)BMI
Probability
0.6
0.4
0.2
0
0
0.5
1.0
1.5
2.0
2.5
3.0
3.5
4.0
BMI ratio
B
Control (PND16-17)
PS amplitude (mV)
20
18
16
12
8
4
0
(-)BMI
(+)BMI
Probability
0.6
0.4
0.2
0
0
0.5
1.0
1.5
2.0
2.5
3.0
3.5
4.0
BMI ratio

Fig.5

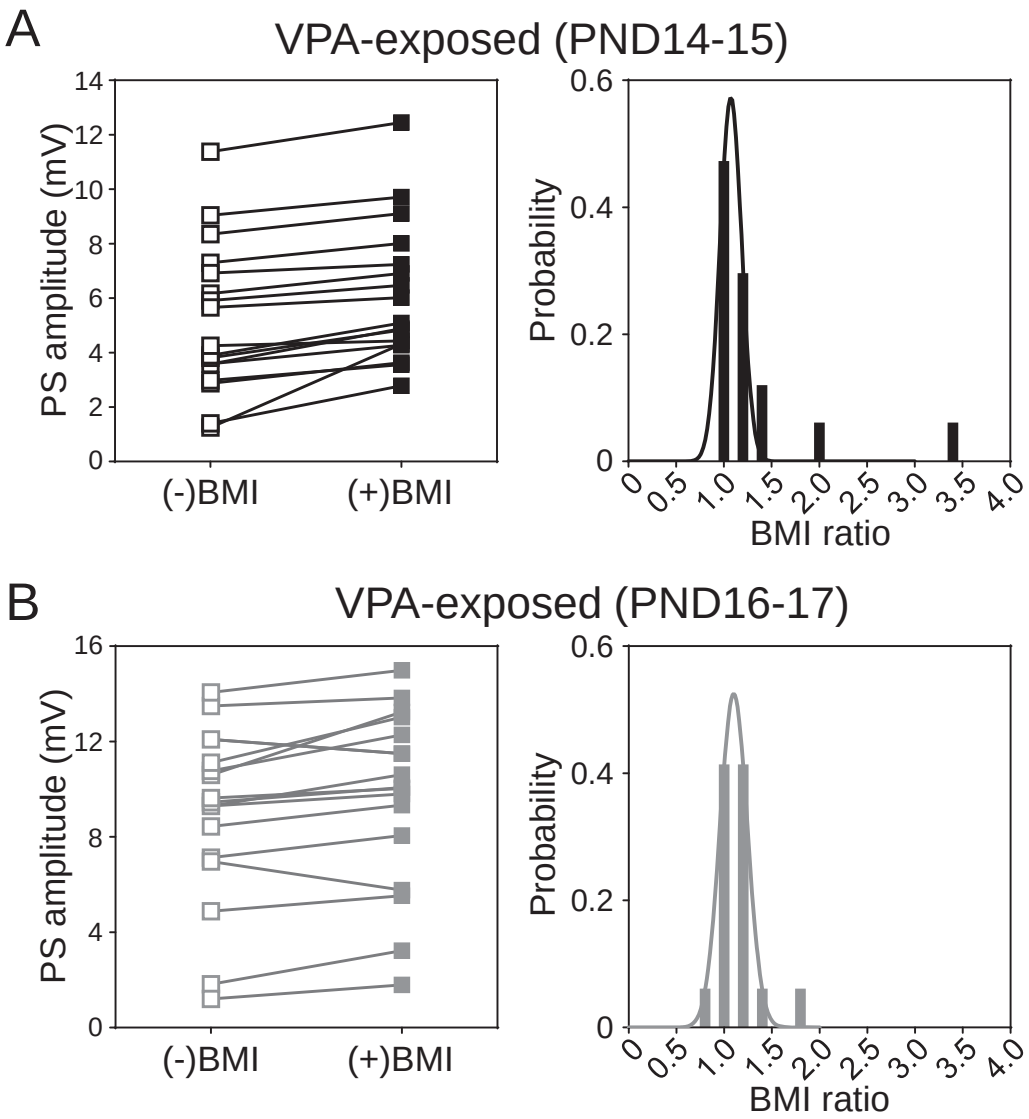
A
VPA-exposed (PND14-15)
PS amplitude (mV)
14
12
10
8
6
4
2
0
(-)BMI
(+)BMI
Probability
0.6
0.4
0.2
0
0
0.5
1.0
1.5
2.0
2.5
3.0
3.5
4.0
BMI ratio
B
VPA-exposed (PND16-17)
PS amplitude (mV)
16
12
8
4
0
(-)BMI
(+)BMI
Probability
0.6
0.4
0.2
0
0
0.5
1.0
1.5
2.0
2.5
3.0
3.5
4.0
BMI ratio

Fig.6

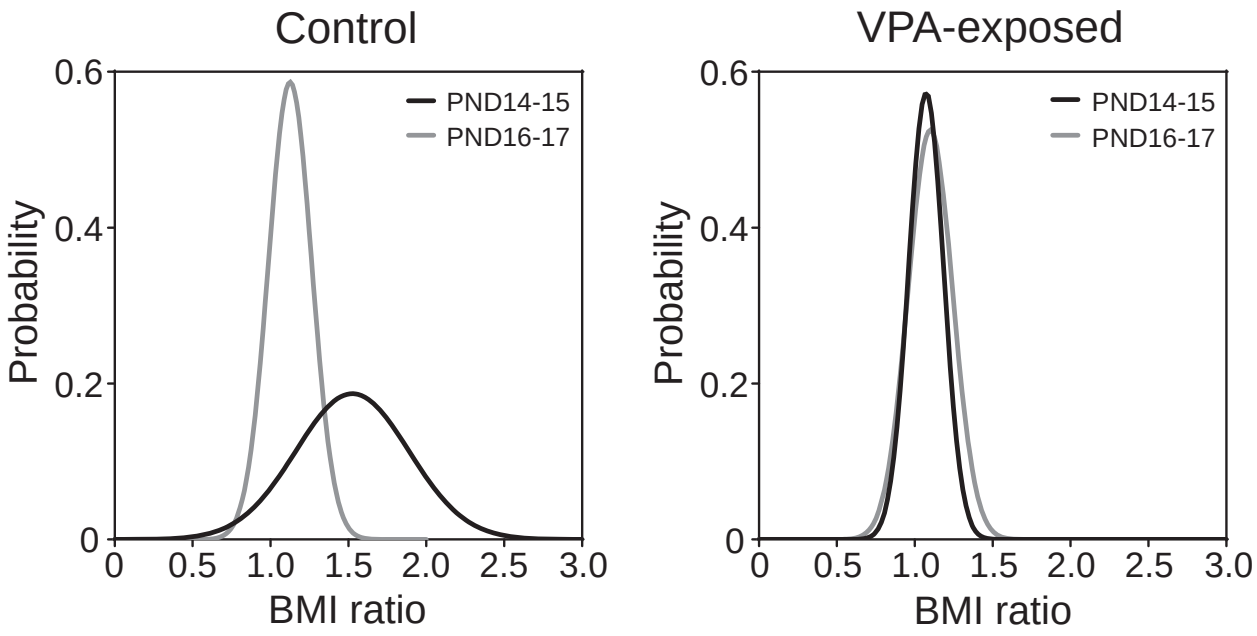
Control
VPA-exposed
PND14-15
PND16-17
Probability
BMI ratio
0
0.2
0.4
0.6
0.5
1.0
1.5
2.0
2.5
3.0

Brief Report

Prenatal Exposure to 1-Bromopropane Causes Delayed Adverse Effects on Hippocampal Neuronal Excitability in the CA1 Subfield of Rat Offspring

Yukiko Fueta[1,*], Toru Ishidao[1], Susumu Ueno[2], Yasuhiro Yoshida[3], Yasunari Kanda[4], Hajime Hori[1]

[1]Department of Environmental Management and Control, School of Health Sciences, University of Occupational and Environmental Health, Kitakyushu, Japan

[2]Department of Occupational Toxicology, University of Occupational and Environmental Health, Kitakyushu, Japan

[3]Department of Immunology and Parasitology, School of Medicine, University of Occupational and Environmental Health, Kitakyushu, Japan

[4]Division of Pharmacology, National Institute of Health Sciences, Tokyo, Japan

For Review Only

*Corresponding Author: Yukiko Fueta, Department of Environmental Management, School of Health Sciences, University of Occupational and Environmental Health, Yahatanishi-ku, Kitakyushu 807-8555, Japan. Tel: +81-93-603-1611. Fax: +81-93-691-2694. E-mail: yukiko@med.uoeh-u.ac.jp.

Running title: Delayed Neurotoxicity in Rats Prenatally Exposed to 10-BP

Number of words in the abstract: 195

Number of words in the text: 2234

Number of figures: 2

Field: Toxicology

For Review Only

Abstract

Objectives: Neurotoxicity of 1-bromopropane (1-BP) has been reported in occupational exposure, but whether the chemical exerts developmental neurotoxicity is unknown. We studied the effects of prenatal 1-BP exposure on neuronal excitability in rat offspring. **Methods:** We exposed dams to 1-BP (700 ppm, 6 h a day for 20 days), and examined hippocampal slices obtained from the offspring at 2, 5, 8, and 13 weeks of age. We measured the stimulation/response (S/R) relationship and paired-pulse ratios (PPRs) of the population spike (PS) at the interpulse intervals (IPIs) of 5 and 10 ms in the CA1 subfield. **Results:** Prenatal 1-BP exposure enhanced S/R relationships of PS at 2 weeks of age; however, the enhancement diminished at 5 weeks of age until it reached control levels. Prenatal 1-BP exposure decreased PPRs of PS at 2 weeks of age. After sexual maturation, however, the PPRs of PS increased at a 50-ms IPI in male rats aged 8 and 13 weeks, and at 50- and 100-ms IPIs in female rats aged 13 weeks. **Conclusions:** Our findings indicate that prenatal 1-BP exposure in dams can cause delayed adverse effects on excitability of pyramidal cells in the hippocampal CA1 subfield of offspring.

Keywords: 1-Bromopropane, Delayed adverse effect, Electrophysiology, Excitability, Prenatal exposure, Rat hippocampal slices

For Review Only

Introduction

Social concerns have been raised regarding the developmental neurotoxicity of prenatally absorbed environmental chemicals, which may exert delayed adverse effects on brain function after birth. It is now recognized that some industrial chemicals (e.g., lead, methylmercury, polychlorinated biphenyls, arsenic, and toluene) can exert developmental neurotoxicity, which results in clinical or subclinical brain dysfunction in humans and in laboratory animals[1]. Many neurotoxic chemicals are present in industrial work settings, and it is not known whether a prenatal exposure to industrial chemicals can cause developmental neurotoxicity.

1-Bromopropane ($CH_3CH_2CH_2Br$; 1-BP), one substitute for specific chlorofluorocarbons, is currently used as a solvent in a variety of industrial and commercial applications. Products containing 1-BP include degreasers and cleaners, spray adhesives, spot removers, coin cleaners, paintable mold release agents, automotive refrigerant flushes, and lubricants[2]. Adverse effects on the central and peripheral nervous system have been found in industrial workers who used 1-BP[3-5]. Adult rats exposed to 1-BP have also shown central neurotoxicity, alteration of mRNA levels of brain neurotransmitter receptors[6], and hippocampal disinhibition caused by a decrease in γ-aminobutyric acid (GABA)-mediated function[7]. In *in vitro* studies using rat hippocampal slices, 1-BP directly suppressed the synaptic plasticity, referred to as a long-term potentiation, in the granule cells of the dentate

https://mc.manuscriptcentral.com/joccuphealth

For Review Only

gyrus[8].

Developmental toxicity is one reason for the threshold limit value set by the American Conference of Governmental Industrial Hygienists for 1,3-BP[9]. We recently reported that prenatal exposure to 1,3-BP suppressed the occurrence of kainite (KA)-induced "wet dog shake" behavior in 20-week-old rat pups[10]. However, whether prenatal 1,3-BP exposure can change neuronal function at the cellular level in the brain of the offspring is unknown. We therefore studied the effects of prenatal 1,3-BP exposure on neuronal excitability after birth. In studying neuronal excitability, population spikes (PS) were recorded in the CA1 subfield of hippocampal slices. For comparison, the same inhalation concentration was used in this study. We analyzed stimulation-dependent responses, stimulation/response (S/R) relationships, and the ratio of responses to double-pulse stimulations, paired-pulse ratios (PPRs). PPRs have been used as a simple method for assessing excitability in neuronal networks[7),11] In this study, we evaluated rats at 2, 5, 8, and 13 weeks of age, to determine whether prenatal 1,3-BP exposure can exert delayed effects after birth.

Materials and Methods

Animals and exposure protocol

Preparation of rats and 1,3-BP inhalation were made according to our previous study[10].

https://mc.manuscriptcentral.com/joccuphealth

For Review Only

Briefly, adult male and female Wistar rats were purchased from Kyudo Co., Ltd. (Tosu, Japan). The rats were housed in plastic cages with paper-made chips (ALPHA-dri, Shepherd Specialty Papers, Richland, MI, USA) on a 12-h light/dark cycle (light period: 7 AM–7 PM). The temperature was controlled at 22–23°C. The relative humidity was approximately 50–70%. The animals had free access to food (CE2, CLEA Japan Inc., Tokyo, Japan) and filtered water (TCW-PPS filter, Advantech Co., Ltd., Tokyo, Japan). Female rats at the proestrus stage were mated with male rats. On the morning of the following day, the existence of sperm in the vaginal plug or vaginal smear was verified as gestation day (GD) 0. 1-BP was purchased from Kanto Chemical Co., Ltd. (Tokyo, Japan). Dams were exposed to 1-BP vapor at a concentration of 700 ppm (6 h/day) for 20 days from GD 1 to GD 20 in an exposure chamber, whereas the other dams were provided fresh air in the same type of chamber. Rats were not allowed access to food and water during the inhalation period. Until the experimental days, male and female rat pups were housed separately after weaning. Some pups in the control and prenatally 1-BP-exposed groups were sourced from pups that were not injected with KA in our previous study[10]. The prenatally 1-BP-exposed groups are abbreviated as the 1-BP group. The number of dams was 15 in the control group and 12 in the 1-BP group. The total number of pups was 34 in the control group and 25 in the 1-BP group.

The experiments were conducted under the guidance of the Ethics Committee of Animal Care and Experimentation in accordance with the Guiding Principle for Animal Care

https://mc.manuscriptcentral.com/joccuphealth

For Review Only

Experimentation, University of Occupational and Environmental Health, Japan, which conforms to the National Institutes of Health Guide for the Care and Use of Laboratory Animals and the Japanese Law for Animal Welfare and Care.

Hippocampal slice preparation

The electrophysiological tests were conducted in male rats at 2, 5, 8, and 13 weeks of age. Female rats were also used for the test at the 13 weeks of age. The female rats at the proestrus stage were deselected for the present experiment, since it is known that estradiol levels can influence the morphology of synaptic boutons and may affect neuron excitability[12]. The total number of tested slices was 135 in the control group and 102 in the 10BP group. The slices were made following previously reported methods[7]. Briefly, the rats were deeply anesthetized with a diethyl ether vapor. After decapitation, the brain was removed and dipped in an ice-cooled artificial cerebrospinal fluid (ACSF) (3–4°C) saturated with an O_2/CO_2 mixture (95%:5%). The ACSF was composed of 124 mM NaCl, 2 mM KCl, 1.25 mM KH_2PO_4, 2 mM $CaCl_2$, 2 mM $MgSO_4$, 26 mM $NaHCO_3$, and 10 mM glucose. The bilateral hippocampi were separated from other brain regions. Next, transverse slices were obtained from the middle third region of the hippocampus with a McIlwain tissue chopper (Mickle Laboratory Engineering, Co., Ltd., Guildford, UK). The thickness of the slice was 600 Lm for 20-week-old rats and 450 Lm for 50, 80, and 130-week-old rats. The slices were transferred to an interface-type recording chamber, which was controlled at 32 ± 0.2°C, and perfused with

For Review Only

ACSF saturated with a mixture of O_2/CO_2 (95%:5%) at a flow rate of 1 ml/min.

All the chemicals used in this study were of reagent grade and purchased from commercial sources.

Stimulation and recordings

After a stabilizing period of 1–2 h, bipolar stimulation electrodes made with stainless steel wires (50 Lm in diameter) were placed on the stratum radiatum, where the Schaffer collateral and commissural fibers run up in the CA1 subfield (Figure 1A). PS was recorded from the pyramidal cell layer in the CA1 subfield using glass microelectrodes (1–2 MN). Stimulations consisted of square0wave pulses (200 Ls) from a stimulator (SEN7203, Nihon Koden Co., Tokyo, Japan) via an isolator (SS202J, Nihon Koden Co.). Stimulation intensities were 10 and 50 LA and increased by 100 LA every 2 min from 100 LA to a current of 600 LA in the slices from the 20week0old rats. In the slices from the 50, 80and 130week0old rats, the stimulation was delivered every 30 sec with intensities of 20, 40, 60, 80, 100, 140, 200, and 300 LA. The S/R relationship in the extracellular recording configuration represents basic excitability of the local area responding to electrical stimulation, and the responses are prefigured to increase as the stimulation strengthens. For the paired0pulse configuration, after the S/R relationship experiment, the current amplitude was adjusted so as to give the almost0maximum PS, 600 LA for slices from the 20week0old rats, and 300 LA for slices from the 50, 80, and 130week0old rats. Interpulse intervals (IPIs) of the paired0pulse stimulation were 5 and 10 ms and delivered

https://mc.manuscriptcentral.com/joccuphealth

For Review Only

every 2 min for slices from the 20-week-old rats and every 1 min for slices from older rats. Electrophysiological signals were amplified with a high-impedance amplifier (Axoclamp 2B, Molecular Devices, Sunnyvale, CA, USA). The signals were then digitized with an AD converter (Digidata 1200, Molecular Devices) and stored on a computer using pCLAMP software (Molecular Devices).

Electrophysiological analysis

PS amplitude was measured as described in our previous study[7] (Figure 1B). Calculation of the PPRs was done as follows:

PPR of PS = second PS amplitude / first PS amplitude

In our previous inhalation studies using adult rats[7], PPRs of PS evoked with paired-pulse stimulation at IPIs of 5 and 10 ms in the CA1 subfield were less than 1 in the hippocampal CA1 of control adult rats, representing the presence of feedback inhibition. Compared to adult rats, PPRs of PS in immature rats can be 1 or higher[13]. Thus, in either case of inhibition or facilitation, paired-pulse configuration in extracellular recordings in the slices is useful to examine the excitability of the local area responding to double-pulse stimulations.

Statistical analysis

Statistical significance was evaluated by a repeated-measure analysis of variance (ANOVA) or an unpaired Welch's *t*-test for a difference between the 10-BP and control groups, when the

https://mc.manuscriptcentral.com/joccuphealth

For Review Only

data were normally distributed. Otherwise, the Mann0Whitney U test was applied. p values < 0.05 (two0tailed) were considered statistically significant. Data represent mean ± standard error of the mean (SEM). Statistical tests were performed in Ekuseru0Toukei 2010 for Windows (Social Survey Research Information Co., Ltd., Tokyo, Japan)

Results

As shown in Figure 1C, the PS amplitude was four times greater in the 10BP group than in the control group at 600 LA of stimulation intensity in 20week0old rats. In 50week0old rats, the enhancement disappeared and the levels decreased to the control level of the S/R relationship of the PS amplitude (Figure 1D). No difference was observed either between the 10BP and control groups at 8 and 13 weeks of age (data not shown). Increased excitability of pyramidal neurons was a transient change.

[Insert Figure 1 here.]

Figure 2A shows examples of paired0pulse responses recorded from the hippocampal CA1 subfield of the control and 10BP groups at 2 weeks of age. As shown in Figure 2B, the averaged PPR was approximately 2 at 2 weeks of age in the control group, suggesting a facilitatory effect. In contrast, inhibition rather than facilitation was observed at the 50ms IPI in the 10BP group. At the 100ms IPI, PPRs showed a slight facilitation, but significantly

https://mc.manuscriptcentral.com/joccuphealth

For Review Only

decreased compared to PPRs in the control group. At 5 weeks of age, PPRs were lower than 0.2, displaying an apparent feedback inhibition in both groups (data not shown), and the effects of prenatal 10BP exposure on PS PPRs disappeared. At 8 and 13 weeks of age, PPRs were still lower than 1, but increased significantly at 5 ms of IPI in the 10BP group compared with the control group (Figures 2C and 2D). In female rats aged 13 weeks, the increase in PPRs was observed at both 100ms and 50ms IPIs (Figure 2E).

[Insert Figure 2 here.]

Discussion

The present study found that prenatal exposure to 10BP enhanced the excitability of CA1 pyramidal neurons and caused a decrease in PPRs of PS amplitude in hippocampal slices from 20week0old rats. The lactation period after birth is considered the period of synaptogenesis in rat brains[14]; so neuronal development during the lactation period may be sensitive to prenatal chemical exposures. In a previous study[10], we reported that prenatal exposure to 10BP suppressed KA0induced "wet dog shake" behaviors in 20week0old rats. Prenatal 10BP exposure rendered the hippocampal CA1 subfield highly responsive to a single stimulation but suppressive to double stimulations. Prenatal 10BP exposure appears to prevent hyperexcitability of CA1 pyramidal neurons induced by repetitive stimulation. Nevertheless,

For Review Only

this is quite different from normal brain development.

Though a decrease in PPRs of PS amplitude was observed in the 10BP group at 2 weeks of age, the difference diminished at 5 weeks of age, as did the S/R relationship. In contrast with the 20week0old pups, the 80and 130week0old groups displayed an increase in PPRs of the PS, termed disinhibition. Thus, prenatal exposure to 10BP can exert developmental effects linked to the excitatory function of neurons and network excitability. Disinhibition has been reported in relation to subclinical and clinical changes in brain excitability in epileptic patients and animals[15], as well as in anxiety disorders[16]. We did not observe any spontaneous abnormal behaviors in the 10BP group during breeding. To date, developmental neurotoxic effects caused by 10BP exposure have not been reported in children whose mothers were exposed occupationally during pregnancy. However, because disinhibition can be related to the hyperexcitable brain and to epilepsy, it should not be concluded that disinhibition is merely a phenomenon restricted to rats. Since disinhibition is interpreted as a disturbance of the excitation/inhibition balance in the hippocampal CA1 area, a disinhibitory effect can be classified as an adverse effect.

The enhancement of excitability induced by prenatal 10BP exposure was observed only in the 20week0old group, and may therefore have been only a transient effect. Alternately, one could argue that the excess basal excitability during synaptogenesis is not coincidental with disinhibition after maturation. If so, the PS S/R relationship can be useful as a new index

https://mc.manuscriptcentral.com/joccuphealth

For Review Only

marker for developmental neurotoxicity of chemicals before the appearance of neurophysiological changes in the brain after maturation. To validate this method for assessing the developmental neurotoxicity of industrial chemicals, we should test chemicals that are already known to exert developmental neurotoxicity. To this end, we are currently investigating valproic acid (VPA), an antiepileptic drug used in an established animal model of the developmental disorder autism[17]. Synaptic transmission generates action potentials; we are also studying field excitatory postsynaptic potentials.

In conclusion, we demonstrated that prenatal 10BP exposure can cause delayed neurotoxicity, although the underlying mechanism is not known yet, and requires further study.

For Review Only

Acknowledgements

We gratefully acknowledge the animal care of K. Egashira. This study was partly supported by the Grants-in-Aid Program of the Japan Society for the Promotion of Science (no. 23510084 to S.U. and no. 18510064 to Y.F.) and a Health and Labour Sciences Research Grant from the Ministry of Health, Labour and Welfare, Japan (to Y.K.).

For Review Only

References

1) Grandjean P, Landrigan P. Developmental neurotoxicity of industrial chemicals. Lancet 2006; 368: 2167-2178.

2) US Environmental Protection Agency: Fact sheet: 1-Bromopropane (1-BP).[Online]. 2016version [cited 2016 Mar 3]; Available from : URL: https://www.epa.gov/assessing-and-managing-chemicals-under-tsca/fact-sheet-1-bromopropane-1-bp#product

3) Ichihara G, Kitoh J, Li W, Ding X, Ichihara S, Takeuchi Y. Neurotoxicity of 1-bromopropane: Evidence from animal experiments and human studies. J Adv Res 2012; 3: 91-98.

4) Samukawa M, Ichihara G, Oka N, Kusunoki S. A case of severe neurotoxicity associated with exposure to 1-bromopropane, an alternative to ozone-depleting or global-warming solvents. Arch Intern Med 2012; 172: 1257-1260.

5) Wang T, Wu M, Wu Y, Tsai W, Lin K, Wang C, et al. Neurotoxicity associated with exposure to 1-bromopropane in golf-club cleansing workers. Clin Toxicol 2015; 53: 823-826.

For Review Only

6) Ueno S, Yoshida Y, Fueta Y, Ishidao T, Liu J, Kunugita N, et al. Changes in the function of the inhibitory neurotransmitter system in the rat brain following subchronic inhalation exposure to 1-bromopropane. Neurotoxicology 2007; 28: 415-420.

7) Fueta Y, Fukuda T, Ishidao T, Hori H. Electrophysiology and immunohistochemistry in the hippocampal CA1 and the dentate gyrus of rats chronically exposed to 1-bromopropane, a substitute for specific chlorofluorocarbons. Neuroscience 2004; 124: 593-603.

8) Kanemitsu M, Fueta Y, Ishidao T, Aou S, Hori H. Development of a direct exposure system for studying the mechanisms of central neurotoxicity caused by volatile organic compounds. Ind Health 2016; 54: 42-49.

9) ACGIH: 1-Bromopropane: TLV(R) Chemical Substances 7th Edition Documentation. [Online]. 2014; Available from : URL: https://www.acgih.org/forms/store/ProductFormPublic/1-bromopropane-tlv-r-chemical-substances-7th-edition-documentation

10) Fueta Y, Kanemitsu M, Egawa S, Ishidao T, Ueno S, Hori H. Prenatal exposure to 1-bromopropane suppresses kainate-induced wet dog shakes in immature rats. J UOEH 2015; 37: 255-261.

11) Waldbaum S, Dudek FE. Single and repetitive paired-pulse suppression: A parametric analysis and assessment of usefulness in epilepsy research. Epilepsia 2009; 50: 904-916.

https://mc.manuscriptcentral.com/joccuphealth

For Review Only

12) .Woolley CS. Effects of estrogen in the CNS. Curr Opin Neurobiol 1999; 9: 3490354.

13) Papatheodoropoulos C, Kostopoulos G. Development of a transient increase in recurrent inhibition and paired0pulse facilitation in hippocampal CA1 region. Dev Brain Res 1998; 108: 2730285.

14) Ben0Ari Y. Developing networks play a similar melody. Trends Neurosci 2001; 24: 3530360.

15) Shumate MD, Lin DD, Gibbs III JW, Holloway KL, A. Coulter D. GABA(A) receptor function in epileptic human dentate granule cells: Comparison to epileptic and control rat. Epilepsy Res 1998; 32: 1140128.

16) Bäckström T, Haage D, Löfgren M, Johansson IM, Strömberg J, Nyberg S, et al. Paradoxical effects of GABA0A modulators may explain sex steroid induced negative mood symptoms in some persons. Neuroscience 2011; 191: 46054

17) Schneider T, Przewłocki R. Behavioral alterations in rats prenatally to valproic acid: Animal model of autism. Neuropsychopharmacology 2005; 30: 80089.

For Review Only

291

292 **Figure legends**

293 **Figure 1 Recording of population spike (PS) from the hippocampal CA1 field and PS**

294 **stimulus/response (S/R) relationships**

295 (A) Stimulation electrode and recording electrode set on the CA1 subfield of the hippocampal

296 slice. The stimulation electrode was set in the stratum radiatum, supplying stimulation to

297 Schaffer collateral and commissural fibers. The PS recording electrode was set in the

298 pyramidal cell layer. (B) Typical PS recorded in the CA1 field of the hippocampal slice

299 obtained from a 20week0old control rat. The thick line represents the PS amplitude

300 measurement. Stimulation intensity was 600 LA. (C) At 2 weeks of age, S/R relationships of

301 the PS amplitude obtained from the 10BP0exposed rats were significantly enhanced compared

302 to S/R relationships in control rats ($p < 0.001$ by repeated0measure ANOVA). (D) At 5 weeks,

303 the enhancement observed in the 10BP0exposed rats disappeared, and the S/R relationship

304 decreased to control levels (PS amplitude: $p = 0.5$ by repeated0measure ANOVA). The

305 horizontal axis represents the stimulation intensity; the vertical axis represents the PS

306 amplitude. Data from 16–19 slices were averaged.

307

308 **Figure 2 Paired-pulse ratios (PPRs) of the population spikes (PSs) evoked with a double**

309 **stimulation of 5 and 10 ms interpulse intervals (IPIs) in the CA1 subfield of hippocampal**

For Review Only

slices obtained from 2-, 8-, and 13-week-old male rats and 13-week-old female rats

(A) Paired-pulse responses evoked with a 600-μA stimulation intensity at 10 ms IPI in the hippocampal CA1 subfield of 20-week-old rats. (B) At 2 weeks of age, PPRs decreased substantially in the 10-BP group (++$p < 0.01$ vs. the control group at the 50-ms IPI, +$p < 0.05$ vs. the control group at the 100-ms IPI by Welch's *t*-test). (C) At 8 weeks of age, PPRs were lower than 1 in both groups, indicating an apparent inhibition. At the 50-ms IPI, the PPR of the 10-BP group increased compared with that of the control group (#$p < 0.05$ by Mann-Whitney U test). (D) Similar to the 50-ms IPI at 8 weeks of age, PPR of male rats in the 10-BP group increased compared with that of the control male rats at 13 weeks of age (+$p < 0.05$ by Welch's *t*-test). (E) At 13 weeks, female rats in the 10-BP group showed an increase in PPRs at 50- and 100-ms IPIs compared with control female rats (##$p < 0.01$ by Mann-Whitney U test; ++$p < 0.01$ by Welch's *t*-test). The horizontal axis represents the IPIs; the vertical axis represents the PPRs of PS amplitude. Data from 16–25 slices were averaged.

For Review Only

Fig. 1

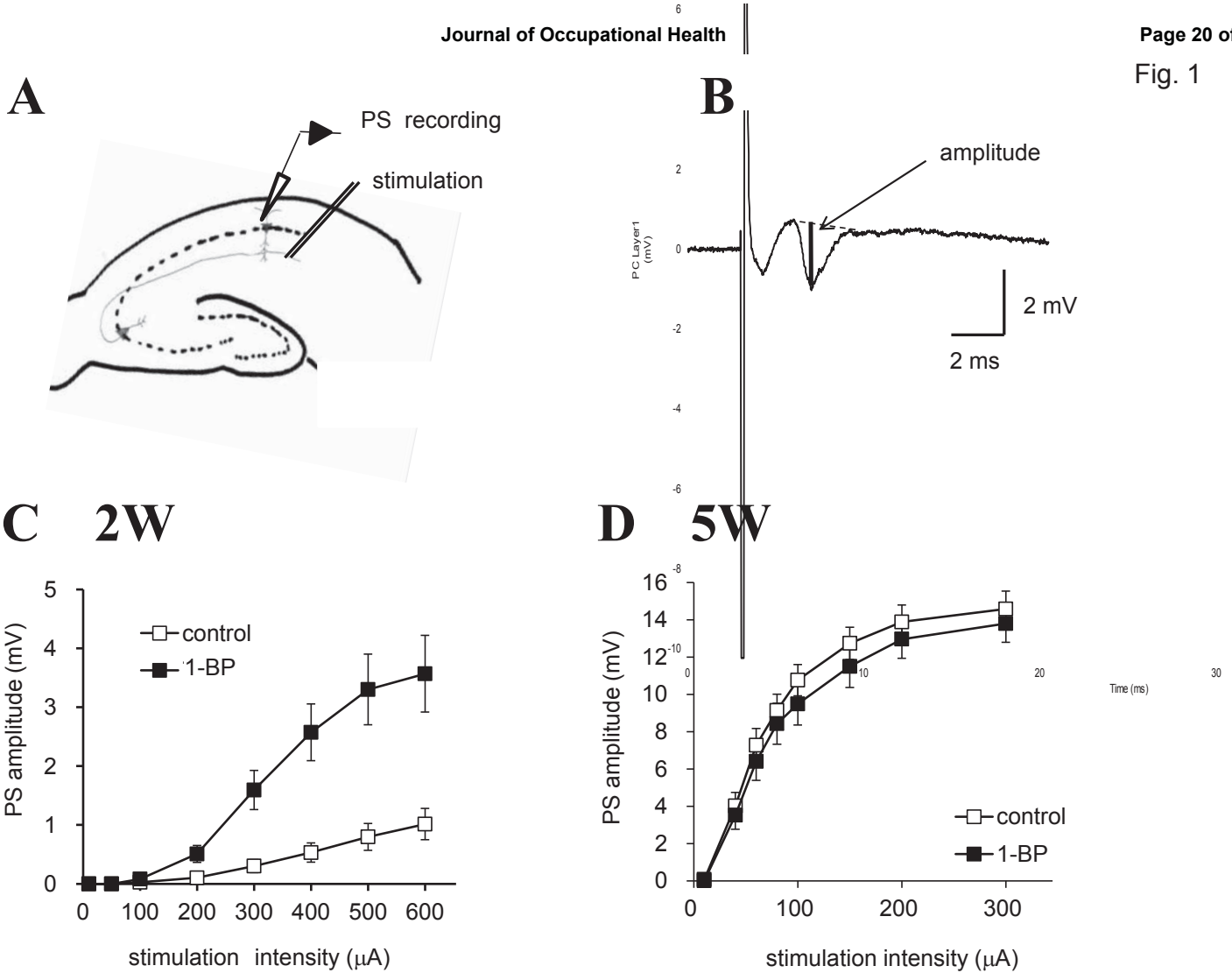
A
PS recording
stimulation
B
amplitude
2 mV
2 ms
PC Layer1 (mV)
C 2W
control
1-BP
PS amplitude (mV)
stimulation intensity (μA)
D 5W
control
1-BP
PS amplitude (mV)
stimulation intensity (μA)
Time (ms)

Fig. 2

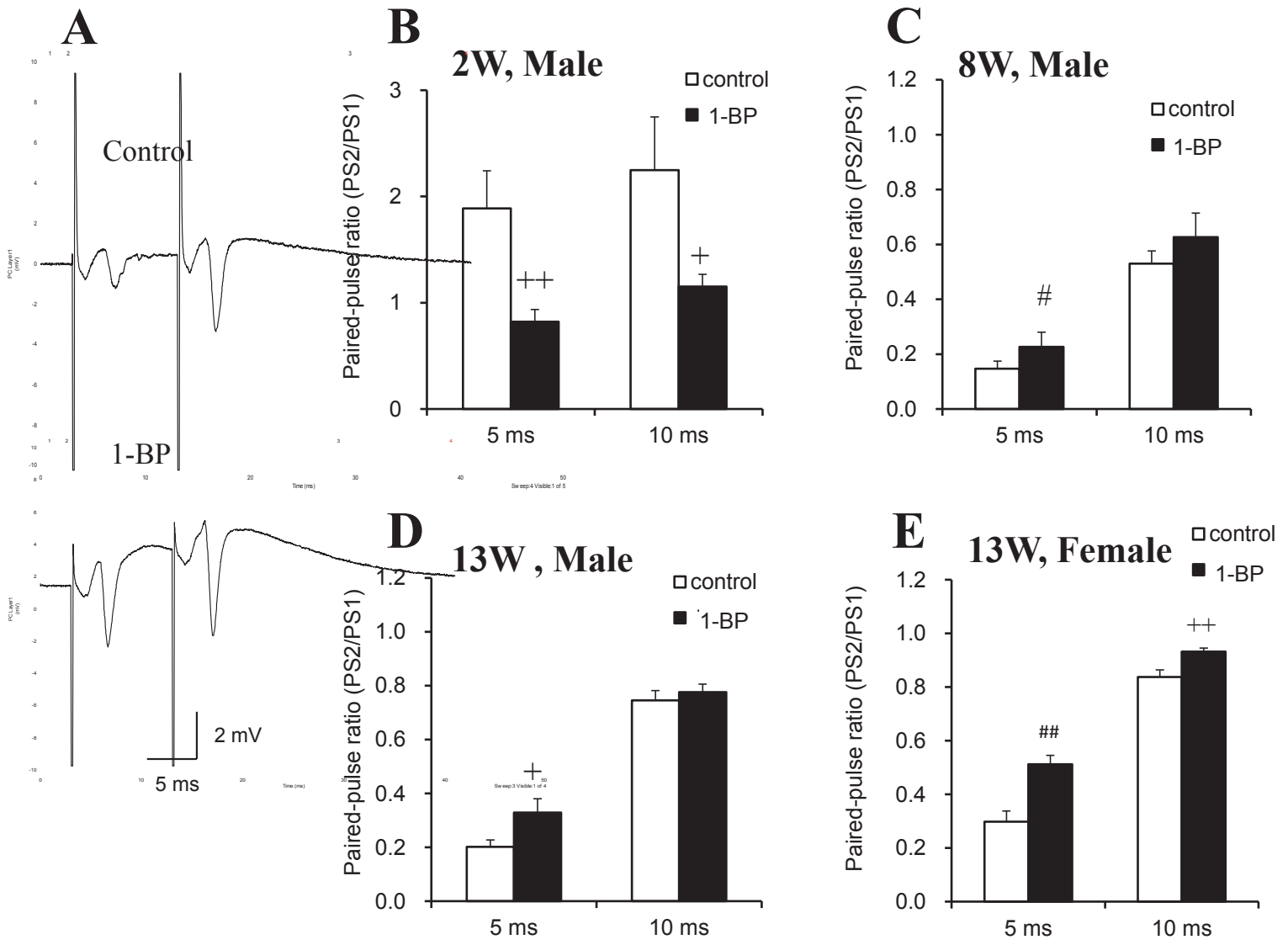
A
Control
1-BP
2 mV
5 ms
B
2W, Male
control
1-BP
Paired-pulse ratio (PS2/PS1)
++
+
5 ms
10 ms
C
8W, Male
control
1-BP
Paired-pulse ratio (PS2/PS1)
#
5 ms
10 ms
D
13W , Male
control
1-BP
Paired-pulse ratio (PS2/PS1)
+
5 ms
10 ms
E
13W, Female
control
1-BP
Paired-pulse ratio (PS2/PS1)
##
++
5 ms
10 ms

Acute exposure to toluene and xylene decrease the expression of connexin43 in human cardiac myocytes

Tomonori Igarashi[a,*], Donald John Wilson[a,b], Susumu Ueno[a]

[a] Department of Occupational Toxicology, Institute of Industrial Ecological Sciences, University of Occupational and Environmental Health Japan, 1-1 Iseigaoka, Yahatanishi-ku, Kitakyushu, 807-8555, Japan

[b] Department of Public Health and Primary Care, College of Medicine, Nursing and Health Sciences, Fiji National University, Lakeba Street, Samabula, Fiji

* Corresponding author:

Tomonori Igarashi

Department of Occupational Toxicology, Institute of Industrial Ecological Sciences, University of Occupational and Environmental Health Japan, 1-1, Iseigaoka, Yahatanishi-ku, Kitakyushu, 807-8555, Japan. Phone: +81-93-691-7404, Fax: +81-93-692-4790, E-mail address: igarashi@med.uoeh-u.ac.jp (T. Igarashi).

ABSTRACT

Organic solvents are widely used in various factories and their use is strictly controlled by official guidelines. Inhalation of organic solvents can cause sudden cardiac death; however, the detailed mechanism of their cardiac toxicity remains unclear. Connexin43 (Cx43) is a principle gap junction protein located in the intercalated disk (IC-D) of cardiac myocytes and associated with a susceptibility to arrhythmia. We hypothesized that acute exposure to organic solvents could affect the expression of gap junction proteins and exposed human cardiac myocytes to doses of toluene and xylene for different times. The cytotoxicity assay revealed that toluene and xylene caused cytotoxicity in a dose-dependent manner. The western blot analysis showed that the expression of Cx43 was significantly decreased after exposure to toluene and xylene (0.56 ± 0.08 AU, $p < 0.05$) in dose-dependent and time-dependent manners. Furthermore, the immunohistochemical study revealed that the expression of Cx43 in the IC-D was significantly decreased and lower in cells that had been exposed to toluene and xylene than it was in the control cells (1.32 ± 0.06AU, $p < 0.05$). Toluene and xylene showed toxic effects on the human cardiac myocytes and decreased the expression of Cx43 in the IC-D.

Keywords: connexin43; toluene; xylene; gap junction protein; cardiotoxicity.

1. Introduction

Organic solvents are widely used in industrial factories and their use is strictly controlled by official guidelines. Several previous studies have reported that organic solvents can affect cardiac function and cause malformations of the heart (Kurppa et al., 1983; Kurppa et al., 1984; Tikkanen and Heinonen, 1991). It has been reported that the early stage following exposure to trichloroethylene is characterized by the induction of atrial and septal defects, whereas chronic exposure to trichloroethylene leads to congestive heart failure (Makwana et al., 2013; Rufer et al., 2010; Watson et al., 2006). Furthermore, trichloromethane (chloroform) has been noted to shorten action potential duration and induce bradycardia and ventricular fibrillation due to the inhibition of multiple ionic currents such as calcium, sodium, and potassium (Tibon-Fisher et al., 1992; Zhou et al., 2011). Another study has reported that inhalation of butane gas causes sudden cardiac death, possibly due to myocardial hypoxia such as is found in the absence of atherosclerotic heart disease (Novosel et al., 2011). Epidemiologic analyses have revealed that a high level of occupational exposure to organic solvents increases the risk of myocardial infarction during at least one year of work. The findings of the abovementioned previous studies imply that organic solvents may affect cardiac function; however, the detailed mechanism of the cardiac toxicity caused by organic solvents remains unclear. As a result, we developed a novel paradigm to understand the relationship between cardiac toxicity and exposure to organic solvents.

Gap junction proteins are expressed in the intercalated disks (IC-Ds) of cardiomyocytes and play an important role in impulse propagation in the heart. Connexin43 (Cx43) is a principle gap junction protein associated with susceptibility to arrhythmia. We have previously reported that the preservation of phosphorylated Cx43 plays an important role in the maintenance of sinus rhythm. In addition, Cx43 gene therapy was noted to recover the cardiac conduction system and prevent ventricular tachycardia in a healed myocardial infarction.

We hypothesized that acute exposure to toluene and xylene would affect the cardiac conduction system in human cardiac myocytes (HCMs). Therefore, we exposed HCMs to different doses of toluene and xylene in order to evaluate the relationship between the cardiotoxicity of each organic solvent and the expression of gap junction proteins.

2. Materials and methods

2.1. Study design

HCMs (PromoCell, Heidelberg, Germany) were plated in a 6-mm well plate according to the manufacturer's instructions. The following day, the cells were exposed to different concentrations of toluene (Nacalai Tesque, Kyoto, Japan) , xylene (Nacalai Tesque), and dimethyl sulfoxide (DMSO), and maintained in 5% CO_2 at 37°C for 3h, 6h, 12h, and 24h. The supernatants were subjected to a cytotoxicity assay, whereas the whole cells were

subjected to western blotting and immunohistochemistry analysis. Toluene and xylene were dissolved in DMSO immediately before use.

2.2. Cytotoxicity assay

The supernatants obtained after exposing the HCMs to the solvents were collected and purified by centrifugation (3000× g for 10 minutes at 20°C). The cytotoxicity assay was performed on the supernatant using ToxiLight® (Lonza, Basel, Switzerland) according to the manufacturer's instructions. Assay of luciferase activity showed a high extracellular level of adenylate kinase, indicating leakage of the latter from the HCMs.

2.3. Western blot analysis

The cardiomyocytes were harvested, homogenized, and dissolved in 0.3 M sucrose/10 mM sodium phosphate buffer containing a protease inhibitor (Roche, Indianapolis, IN, USA) and a phosphatase inhibitor (Sigma, St. Louis, MO, USA). Next, centrifugation (3000× g for 10 minutes at 4°C) was performed to obtain the cell lysates. Protein concentrations were then determined by the bicinchoninic acid assay (Thermo Scientific, Rockford, IL, USA). The proteins were fractionated by sodium dodecyl sulfate polyacrylamide gel electrophoresis, transferred to nitrocellulose membranes, blocked with 3% non-fat dry milk, and blotted with anti-Cx43 (Thermo Scientific), anti-human ether-a-go-go related gene (HERG) (Invitrogen,

Carlsbad, CA, USA), anti-Nav1.5 (Santa Cruz Biotechnology, Dallas, TX, USA), anti-L-type Ca^{2+} (Santa Cruz Biotechnology), and anti-actin (Santa Cruz Biotechnology) at 4°C overnight. The following day, the membranes were washed with blocking buffer and incubated with secondary antibodies conjugated with horseradish peroxidase. Protein bands were detected by enhanced chemiluminescence (Thermo Scientific) and quantified using the ImageJ software (National Institutes of Health (NIH), Bethesda, MD, USA). The band intensity for each protein was normalized to the intensity of actin in its lane.

2.4. Immunohistochemical analysis

Cover glasses were placed on the bottoms of 6-well plates before plating the HCMs. Twenty four hours after exposing the cells to toluene and xylene, the HCMs on the cover glasses were subjected to an immunohistochemical study. The HCMs were fixed in 2% formalin, followed by washing with phosphate-buffered saline (3 times, 5 minutes each). The cells were then incubated overnight with anti-Cx43 antibodies (1:400 dilution, Invitrogen) at 4°C overnight. The following day, the cells were incubated with fluorescein isothiocyanate-conjugated goat anti-rabbit IgG (1:400 dilution; Jackson ImmunoResearch Laboratories, Inc., West Grove, PA) before being examined by laser microscopy (×20 magnification; Axio; Carl Zeiss, Oberkochen, Germany). The signal intensities of the connexin proteins in the IC-D and lateral membrane were digitized and quantified using the Image-J software.

2.5. Statistical analysis

Statistical differences were determined by repeated measures analysis of variance. All the analyses were conducted at a 0.05 significance level. Data are presented as mean ± standard deviation.

3. Results

3.1. Cytotoxic effects of toluene and xylene on HCMs

The HCMs were exposed to 0μM, 3.1μM, 6.3μM, 12.5μM, 25.0μM, and 50.0μM of toluene and xylene for 24 hours and subjected to a cytotoxicity assay as described above. The supernatants from the HCMs were used in a cytotoxicity evaluation according to the ToxiLight® assay. We found that the cytotoxicity of each solvent increased in a concentration-dependent manner (Fig. 1). In addition, the two solvents were significantly and more cytotoxic to the HCMs [xylene at 25 μM (24.3 ± 19.5 IU, $p < 0.01$) and 50 μM (288.7 ±13.5 IU, $p < 0.01$), toluene at 50 μM (250.3 ± 8.39 IU, $p < 0.01$)] than DMSO was. Overall, xylene showed a higher cytotoxic effect than toluene did (half maximal inhibitory concentration values: xylene, 21 μM; toluene, 38 μM). Therefore, we used toluene and xylene at 10 μM and 20 μM, respectively, for the subsequent western blotting and immunohistochemical studies.

3.2. Western blot analyses of Cx43 expression in HCMs exposed to toluene and xylene

We assessed Cx43 expression by western blot analysis using an anti-Cx43 antibody that recognized total Cx43. The expression of Cx43 was decreased in a dose-dependent manner after exposure of the cells to toluene and xylene (Fig. 2A). The signal intensity was quantified using the ImageJ software and normalized to the expression of actin in the non-treated cells. We found that there were significant reductions in Cx43 expression when toluene was used at concentrations of 2 μM (0.58 ± 0.03 AU, $p < 0.05$) and 20 μM (0.38 ± 0.04 AU, $p < 0.01$) and xylene was used at 1 μM (0.59±0.12 AU, $p < 0.01$) and 10 μM (0.49 ± 0.07 AU, $p < 0.01$) (Fig. 2B). Next, we performed a time-course cytotoxic evaluation of the organic solvents. It was observed that the expression of Cx43 decreased in a time-dependent manner after the cells were exposed to either toluene or xylene (Fig. 3A). Furthermore, we found that, compared to the non-treated cells, there were significant reductions in Cx43 expression after incubation of the cells with toluene for 12 hours (0.56 ± 0.05 AU, $p < 0.05$) or 24 hours (0.42 ± 0.03 AU, $p < 0.01$), as well as with xylene for 12 hours (0.46 ± 0.02 AU, $p < 0.01$) or 24 hours (0.51 ± 0.07 AU, $p < 0.01$) (Fig. 3B).

3.3. Immunohistochemical analyses of Cx43 expression in HCMs exposed to toluene and xylene

We evaluated the percentage expression of Cx43 in the IC-Ds using immunohistochemistry. Representative pictures showing cells stained with Cx43 antibody are

shown in Fig. 4A. We found that there were significant reductions in Cx43 expression in the IC-Ds when toluene was used at concentrations of 0.2 μM (0.73 ± 0.06 AU, $p < 0.05$), 2 μM (0.64 ± 0.04 AU, $p < 0.05$), and 20 μM (0.45 ± 0.14 AU, $p < 0.01$), and xylene was used at 1 μM (0.65 ± 0.06 AU, $p < 0.05$) and 10 μM (0.59 ± 0.07 AU, $p < 0.05$). This suggests that the organic solvents possibly affect the trafficking pathway of Cx43 proteins (Fig. 4B).

3.4. Western blot analyses of HERG, Nav1.5, and L-type Ca^{2+} channel expressions in HCMs exposed to toluene and xylene

We also assessed the expression of major cardiac channels such as HERG, Nav1.5, and L-type Ca^{2+} using western blot analysis, because these channel proteins play an important role in action potential duration. We found that the expressions of the channels before and after exposure of the cells to toluene or xylene for 24 hours were the same (Fig. 5).

4. Discussion

The National Institute for Occupational Safety and Health has declared the criteria for the use of organic solvents in order to prevent disease and hazardous conditions at the workplace (https://www.cdc.gov/niosh/topics/organsolv/). The criteria include all the information on an organic solvent, which is necessary to know at the workplace. Although the usage of organic solvents are strictly controlled by official guidelines, workers are likely to be exposed to high

concentrations of organic solvents, especially in a narrow space. The inhalation of organic solvents sometimes causes sudden death. The main mechanism underling the lethality of organic solvents is considered to be oxygen deficiency in cardiomyocytes (Harrison et al., 2016); however, the detailed mechanism remains unknown. Butane is a typical organic solvent used in industries and that sometimes causes sudden death (Celinski et al., 2013; Novosel et al., 2011). According to our cytotoxicity assay, toluene and xylene showed cytotoxic effects on the HCMs in dose-dependent and time-dependent manners, which suggests that the organic solvents have acute cytotoxic effects on human cardiomyocytes. Furthermore, environmental chemical contamination is a risk factor for congenital heart disease, which indicates that exposure to chemicals poses a risk for defective heart function during the embryonic stage (Rufer et al., 2010; Tikkanen and Heinonen, 1991). Although several epidemiological studies have been focused on the effects of chronic or constant exposure to organic solvents at the workplace (Kotseva and Popov, 1998; Tibon-Fisher et al., 1992), it would also be highly important to assess acute cell damage in the human heart caused by such exposures. The next step would then be an animal experiment to reveal how organic solvents might affect the conduction system in the heart *in vivo*. Several studies have reported that nanoparticles showed direct and indirect toxic effects on the cardiovascular system and increased the risks of ischemic heart disease or cerebrovascular disease (Chen et al., 2015; Nelin et al., 2012; Polichetti et al., 2009), and furthermore demonstrated that

mortality would be decreased at workplaces where workers are constantly exposed to small particles in the air (Stephan et al., 2014; Toren et al., 2007). However, little is known about the mortality of workers at places where high concentrations of organic solvents are used. According to our results, toluene and xylene are toxic to HCMs, however, it is quite important to evaluate the mechanism of cytotoxic effects of organic solvents on HCMs.

Furthermore, we assessed the relationship between exposure to organic solvent and connexin expression in HCMs. According to our results, toluene and xylene decreased the expression of gap junction proteins, increased the heterogeneity of cardiac propagation, and caused reentrant arrhythmias such as ventricular tachycardia and ventricular fibrillation. Imbalance in autonomic nerve activities has been stated as another important factor that increases the risk of arrhythmia (Matikainen and Juntunen, 1985; Morrow and Steinhauer, 1995; Murata et al., 1994). Since autonomic nerve activities are influenced by organic solvents following a long-term occupational exposure (Morrow and Steinhauer, 1995), high concentrations of organic solvents might drive sympathetic nerve activities. We have previously shown that an altered expression of Cx43 is strongly associated with heterogeneity of cardiac impulse propagation in atrial fibrillation (AF) in healed myocardial infarction models (Bikou et al., 2011; Greener et al., 2012; Igarashi et al., 2012). In the present study, we found that the expression of Cx43 was significantly decreased by toluene and xylene in dose-dependent and time-dependent manners after exposing HCMs to the solvents. These

results imply that a decreased expression of Cx43 slows impulse propagation in cardiomyocytes and increases the risk of arrhythmia.

Connexin proteins are folded in the Golgi system, which are phosphorylated and trafficked to the plasma membrane surface (Basheer and Shaw, 2016; Falk et al., 2016; Zhang and Shaw, 2014). We have previously shown that the expression of connexin proteins is significantly decreased in AF induced by atrial burst-pacing in animal models (Igarashi et al., 2012). According to our immunohistochemical analyses, lateralized expression of Cx43 was significantly increased after exposing the cells to toluene and xylene, indicating that the organic solvents affect the intracellular trafficking of connexin proteins. Since we observed that the expression of connexin proteins in the IC-D was decreased by the organic solvents, there are possibilities that the organic solvents would affect the phosphorylation status of connexin proteins. Several previous studies have reported that chemical agents affect the trafficking of proteins such as sodium and potassium channels (Abriel et al., 2015; Basheer and Shaw, 2016; Steffensen et al., 2015). However, no organic solvents have been reported to affect the expression of gap junction proteins. Another concern is whether organic solvents might affect the functions of phosphatases and/or phosphatase inhibitors in cardiomyocytes. Therefore, further investigations are necessary to assess the relationship between exposure to organic solvents and the phosphorylation system in cardiomyocytes.

According to official reports from the Centers for Disease Control and Prevention, nine

sudden deaths have been caused by inhalation of hydrocarbon gases and oxygen deficiency at specific locations such as catwalk or in front of an open hatch, where the oxygen level might have been low (Harrison et al., 2016). Most of the reasons for sudden deaths in such places are due to oxygen deficiency; however, a direct effect of organic solvents on HCMs can cause sudden death especially at workplaces where organic solvents are used. We have shown that toluene and xylene had cytotoxic effects on the HCMs in the acute phase; however, further studies should be carried out to assess the effects of long-term continuous exposure to organic solvents at low concentrations. Since the concentration of organic solvents in the air is strictly controlled by official guidelines, it is highly unlikely that workers would inhale high concentrations of organic solvents for long periods. Moreover, organic solvents can directly decrease the expression of Cx43, as well as decrease impulse propagation and increase the risk of arrhythmia. AF is the most common arrhythmia in clinical practice with a prevalence rate of about 10% in individuals aged > 80 years old (Alonso and Norby, 2016; Ko et al., 2016). The major contributing factor to AF is thought to be the age of patients; however, other risk factors for AF include hypertension, dyslipidemia, and diabetes mellitus. In clinical medical practice, little is known about the relationship between continuous exposure to organic solvents and the occurrence of AF. Since the prevalence of AF is strongly correlated with patient age, we have not assessed to the working history or working environmental aspects when patients with AF come to the hospital. Therefore, the work history and working

conditions of a patient who presents with AF must be evaluated. Furthermore, the direct effects of continuous and low-dose exposure of organic solvents on the human heart have to be evaluated in large animal models. This will allow for the investigation of exposure to low doses of organic solvents and the resulting long-term effects on cardiomyocytes.

In conclusion, toluene and xylene showed cytotoxic effects on HCMs in dose-dependent and time-dependent manners. In addition, toluene and xylene decreased the expression of Cx43, especially that in the IC-Ds of the HCMs. An *in vivo* electrophysiological study would be necessary to understand the mechanism underlying the toxicities of the organic solvents and how they increase susceptibility to arrhythmia.

Acknowledgements

We thank Rie Yukiya for secretarial assistance.

Conflict of interest

The authors declare that there are no conflicts of interest.

Funding information

This work was funded by the Occupational Research Fund of the University of Occupational and Environmental Health, School of Medicine, Japan.

References

Abriel, H., Rougier, J.S., Jalife, J., 2015. Ion channel macromolecular complexes in cardiomyocytes: roles in sudden cardiac death. Circ. Res. 116, 1971–1988.

Alonso, A., Norby, F.L., 2016. Predicting atrial fibrillation and its complications. Circ. J. 80, 1061–1066.

Basheer, W.A., Shaw, R.M., 2016. Connexin 43 and CaV1.2 ion channel trafficking in healthy and diseased myocardium. Circ. Arrhythm. Electrophysiol. 9, e001357.

Bikou, O., Thomas, D., Trappe, K., Lugenbiel, P., Kelemen, K., Koch, M., Soucek, R., Voss, F., Becker, R., Katus, H.A., Bauer, A., 2011. Connexin 43 gene therapy prevents persistent atrial fibrillation in a porcine model. Cardiovasc. Res. 92, 218–225.

Celiński, R., Skowronek, R., Uttecht-Pudełko, A., 2013. [Atypical case of teenager fatal poisoning by butane as a result of gas for lighters inhalation against his will]. Przegl. Lek. 70, 473–475.

Chen, Z., Wang, Y., Zhuo, L., Chen, S., Zhao, L., Luan, X., Wang, H., Jia, G., 2015. Effect of titanium dioxide nanoparticles on the cardiovascular system after oral administration. Toxicol. Lett. 239, 123–130.

Falk, M.M., Bell, C.L., Kells Andrews, R.M., Murray, S.A., 2016. Molecular mechanisms regulating formation, trafficking and processing of annular gap junctions. BMC Cell Biol. 17 Suppl 1, S22.

Greener, I.D., Sasano, T., Wan, X., Igarashi, T., Strom, M., Rosenbaum, D.S., Donahue, J.K., 2012. Connexin43 gene transfer reduces ventricular tachycardia susceptibility after myocardial infarction. J. Am. Coll. Cardiol. 60, 1103–1110.

Harrison, R.J., Retzer, K., Kosnett, M.J., Hodgson, M., Jordan, T., Ridl, S., Kiefer, M., 2016. Sudden deaths among oil and gas extraction workers resulting from oxygen deficiency and inhalation of hydrocarbon gases and vapors - United States, January 2010-March 2015. MMWR Morb. Mortal. Wkly. Rep. 65, 6–9.

Igarashi, T., Finet, J.E., Takeuchi, A., Fujino, Y., Strom, M., Greener, I.D., Rosenbaum, D.S., Donahue, J.K., 2012. Connexin gene transfer preserves conduction velocity and prevents atrial fibrillation. Circulation 125, 216–225.

Ko, D., Rahman, F., Schnabel, R.B., Yin, X., Benjamin, E.J., Christophersen, I.E., 2016. Atrial fibrillation in women: epidemiology, pathophysiology, presentation, and prognosis. Nat. Rev. Cardiol. 13, 321–332.

Kotseva, K., Popov, T., 1998. Study of the cardiovascular effects of occupational exposure to organic solvents. Int. Arch. Occup. Environ. Health. 71 Suppl, S87–S91.

Kurppa, K., Hietanen, E., Klockars, M., Partinen, M., Rantanen, J., Rönnemaa, T., Viikari, J., 1984. Chemical exposures at work and cardiovascular morbidity. Atherosclerosis, ischemic heart disease, hypertension, cardiomyopathy and arrhythmias. Scand. J. Work Environ. Health 10, 381–388.

Kurppa, K., Holmberg, P.C., Hernberg, S., Rantala, K., Riala, R., Nurminen, T., 1983. Screening for occupational exposures and congenital malformations. Scand. J. Work Environ. Health 9, 89–93.

Makwana, O., Ahles, L., Lencinas, A., Selmin, O.I., Runyan, R.B., 2013. Low-dose trichloroethylene alters cytochrome P450-2C subfamily expression in the developing chick heart. Cardiovasc. Toxicol. 13, 77–84.

Matikainen, E., Juntunen, J., 1985. Autonomic nervous system dysfunction in workers exposed to organic solvents. J. Neurol. Neurosurg. Psychiatry 48, 1021–1024.

Morrow, L.A., Steinhauer, S.R., 1995. Alterations in heart rate and pupillary response in persons with organic solvent exposure. Biol. Psychiatry 37, 721–730.

Murata, K., Araki, S., Yokoyama, K., Yamashita, K., Okajima, F., Nakaaki, K., 1994. Changes in autonomic function as determined by ECG R-R interval variability in sandal, shoe and leather workers exposed to n-hexane, xylene and toluene. Neurotoxicology 15, 867–875.

Nelin, T.D., Joseph, A.M., Gorr, M.W., Wold, L.E., 2012. Direct and indirect effects of particulate matter on the cardiovascular system. Toxicol. Lett. 208, 293–299.

Novosel, I., Kovačić, Z., Gusić, S., Batelja, L., Nestić, M., Seiwerth, S., Skavić, J., 2011. Immunohistochemical detection of early myocardial damage in two sudden deaths due to intentional butane inhalation. Two case reports with review of literature. J.

Forensic Leg. Med. 18, 125–131.

Polichetti, G., Cocco, S., Spinali, A., Trimarco, V., Nunziata, A., 2009. Effects of particulate matter (PM(10), PM(2.5) and PM(1)) on the cardiovascular system. Toxicology 261, 1–8.

Rufer, E.S., Hacker, T.A., Flentke, G.R., Drake, V.J., Brody, M.J., Lough, J., Smith, S.M., 2010. Altered cardiac function and ventricular septal defect in avian embryos exposed to low-dose trichloroethylene. Toxicol. Sci. 113, 444–452.

Steffensen, A.B., Refaat, M.M., David, J.P., Mujezinovic, A., Calloe, K., Wojciak, J., Nussbaum, R.L., Scheinman, M.M., Schmitt, N., 2015. High incidence of functional ion-channel abnormalities in a consecutive long QT cohort with novel missense genetic variants of unknown significance. Sci. Rep. 5, 10009.

Stephan, C., Schlawne, C., Grass, S., Waack, I.N., Ferenz, K.B., Bachmann, M., Barnert, S., Schubert, R., Bastmeyer, M., de Groot, H., Mayer, C., 2014. Artificial oxygen carriers based on perfluorodecalin-filled poly(n-butyl-cyanoacrylate) nanocapsules. J. Microencapsul. 31, 284–292.

Tibon-Fisher, O., Heller, E., Ribak, J., 1992. [Occupational scleroderma due to organic solvent exposure]. Harefuah 122, 530-2, 551.

Tikkanen, J., Heinonen, O.P., 1991. Risk factors for ventricular septal defect in Finland. Public Health 105, 99–112.

Torén, K., Bergdahl, I.A., Nilsson, T., Järvholm, B., 2007. Occupational exposure to particulate air pollution and mortality due to ischaemic heart disease and cerebrovascular disease. Occup. Environ. Med. 64, 515–519.

Watson, R.E., Jacobson, C.F., Williams, A.L., Howard, W.B., DeSesso, J.M., 2006. Trichloroethylene-contaminated drinking water and congenital heart defects: a critical analysis of the literature. Reprod. Toxicol. 21, 117–147.

Zhang, S.S., Shaw, R.M., 2014. Trafficking highways to the intercalated disc: new insights unlocking the specificity of connexin 43 localization. Cell Commun. Adhes. 21, 43–54.

Zhou, Y., Wu, H.J., Zhang, Y.H., Sun, H.Y., Wong, T.M., Li, G.R., 2011. Ionic mechanisms underlying cardiac toxicity of the organochloride solvent trichloromethane. Toxicology. 290, 295–304.

Figure legends

Fig. 1. Evaluation of the cytotoxic effects of toluene and xylene on human cardiac myocytes (HCMs).

HCMs were exposed to different concentrations of toluene, xylene, and dimethyl sulfoxide (DMSO). Luciferase activity was used to evaluate the cytotoxicities of the solvents using ToxiLight® assay.

Fig. 2. Western blot analysis of connexin43 (Cx43) expression in human cardiac myocytes (HCMs) exposed to toluene and xylene.

HCMs were exposed to different concentrations of toluene and xylene for 24 hours. (A) Whole cell lysates were then harvested and subjected to western blot analysis. (B) The expression levels of Cx43 and actin were quantified and normalized to the expression level of actin in control cells.

Fig. 3. Time-course evaluation of connexin43 (Cx43) expression in human cardiac myocytes (HCMs) exposed to toluene and xylene using western blot analysis.

HCMs were exposed to toluene (20 μM) or xylene (10 μM) for 3, 6, 12, or 24 hours. (A) Whole cell lysates were harvested and subjected to western blot analysis. (B) The expression levels of Cx43 and actin were quantified and normalized to the expression level of actin in

control cells.

Fig. 4. Immunohistochemical analysis of connexin43 (Cx43) expression in human cardiac myocytes (HCMs) exposed to toluene and xylene.

HCMs were exposed to different concentrations of toluene and xylene for 24 hours. (A) Representative images of cells stained with Cx43 antibody. The yellow boxes are magnified images of intercalated discs (IC-Ds) located between neighboring cardiomyocytes. The red arrow indicates Cx43 expressed in the IC-Ds. The expression of Cx43 in all fields and IC-Ds was quantified using the ImageJ software. (B) The expression level of Cx43 in the IC-Ds.

Fig. 5. Western blot analysis of human ether-a-go-go related gene (HERG), Nav1.5, and L-type Ca^{2+} channel expressions in human cardiac myocytes (HCMs) exposed to toluene and xylene.

HCMs were exposed to toluene (20 μM) or xylene (10 μM) for 24 hours. Whole cell lysates were then harvested and subjected to western blot analysis using primary antibodies against HERG, Nav1.5, L-type Ca^{2+}, and actin.